5-1-2010

Accelerated Aging Study of Machine Winding Insulation under AC and High Frequency Pulse Voltage Application

Sajal Raj Chalise

ACCELERATED AGING STUDY OF MACHINE WINDING INSULATION UNDER AC AND HIGH FREQUENCY PULSE VOLTAGE APPLICATION

By

Sajal Raj Chalise

A Thesis
Submitted to the Faculty of
Mississippi State University
in the Partial Fulfillment of the Requirements
for the Degree of Master of Science
in Electrical Engineering
in the Department of Electrical and Computer Engineering

Mississippi State, Mississippi

May 2010

ACCELERATED AGING STUDY OF MACHINE WINDING INSULATION UNDER AC AND HIGH FREQUENCY PULSE VOLTAGE APPLICATION

By

Sajal Raj Chalise

Approved:

Stanislaw Grzybowski Professor of Electrical and Computer Engineering Department Director, High Voltage Laboratory (Major Advisor)	Nicolas H. Younan Professor and Head of Electrical and Computer Engineering Department (Committee Member)
Herbert L. Ginn Associate Professor of Electrical and Computer Engineering Department (Committee Member)	James E. Fowler Professor and Graduate Program Director of Electrical and Computer Engineering Department (Graduate Coordinator)
Sarah A. Rajala Dean, Bagley College of Engineering	

Name: Sajal Raj Chalise

Date of Degree: 01 May 2010

Institution: Mississippi State University

Major Field: Electrical Engineering

Major Professor: Stanislaw Grzybowski

Title of Study: ACCELERATED AGING STUDY OF MACHINE WINDING INSULATION UNDER AC AND HIGH FREQUENCY PULSE VOLTAGE APPLICATION

Pages in Study: 97

Candidate for Degree of Master of Science

It is common practice to perform accelerated aging with 60 Hz ac to determine the lifetime characteristics of insulation used in the machine. Comparable breakdown measurements are performed at different voltage levels and temperatures for the polyimide insulated machine winding under normal operating conditions of 60 Hz ac. The result shows that the time to failure can be represented by the inverse power law and the Arrhenius equation with respect to test voltage and temperature respectively.

However, the use of power electronic devices causes harmonics, and spikes that electrically degrade the machine winding insulation. Applied high frequency pulse voltages can be used to study the impact of electrical degradation of the machine winding insulation that exists in electrical machines. Evaluation of change in dielectric strength, partial discharge and breakdown voltage is monitored versus aging caused by high frequency pulse voltage at 90% of operating temperature.

DEDICATION

I would like to dedicate this research work to my beloved parents, Mr. Surendra Chalise and Mrs. Shova Chalise for their love, and my advisor Dr. Stanislaw Grzybowski for his continuous support.

ACKNOWLEDGEMENTS

I take great pleasure in expressing my gratitude and sincere thanks to my academic advisor, Dr. Stanislaw Grzybowski, for his valuable guidance and support that enabled me to complete my research work in the stipulated time. I would also like to thank Dr. Nicolas Younan and Dr. Herbert Ginn for their advice and being a part of my thesis committee. I also take this opportunity to express my thanks to Dr. Erling Ilstand, visiting professor for his suggestions regarding ac voltage test. I am thankful for Dr. Clay Taylor, who helped me setup the instruments required for the research study. I am expressing my thanks to Mr. Jason Pennington, technician, and all the graduate students of the High Voltage Laboratory at Mississippi State University for their assistance and co-operation during the course of my research.

Finally, I would like to thank the Office of Naval Research (ONR) for providing financial support to Mississippi State University to carry out the research work. This research project has been sponsored by ONR Funds: N00014-02-1-0623, Electric Ship Research Development and Consortium (ESRDC).

TABLE OF CONTENTS

LIST OF TABLES

LIST OF FIGURES

DEFINITION

a) Machine winding: An insulated copper (or aluminum) electrical conductor used in motors, transformers, and other electromagnetic equipment.

b) Machine winding Insulation: The common insulation used for the machine windings are polyurethane, polyimide, polyester, and polyamideimide. They are all characterized by having higher dielectric strength and good thermal resistant property, capable of running the machine in severe conditions (thermal, electrical, and mechanical stress).

c) Accelerated Aging: The aging of machine winding insulation with voltage and temperature higher than normal operating condition.

d) Electrical Breakdown: A discharge that completely bridges the insulation during electrical testing and reducing the voltage between the electrodes practically to zero.

e) High Frequency Pulse Voltage: The square pulse voltage with the frequency range of 20 kHz to 40 kHz to carry out accelerated aging.

f) Partial Discharge: A localized electrical discharge that only partially bridges the insulation between conductors and which can or cannot occur adjacent to a conductor.

g) Partial Discharge Inception Voltage (PDIV): The increased minimum value of voltage when partial discharges attain, or exceed, a specified low magnitude.

h) Partial Discharge Extinction Voltage (PDEV): The gradually - reduced voltage values at which the partial discharges become less than the same specified magnitude.

i) Time to breakdown: The time required to obtain electrical breakdown of insulation under accelerated aging condition.

j) Weibull distribution: A life-distribution model used for the time-to-failure model of electrical insulation.

CHAPTER I

INTRODUCTION

1.1 Objective of Study

Polyimide is one of the most heat resistant polymers with high electric breakdown strength, good mechanical properties, and good chemical resistance. Polyimide is used in severe environmental conditions and its uses are becoming increasingly popular [1]. Polyimide is commonly applied as electrical insulation in a fine gauge of inverter-fed motor windings and in high voltage coils of encapsulated fly-back transformers. In such devices, the wire insulation may be exposed to high temperatures, various power frequencies, and transient voltage waveforms. In random–wound machines, partial discharges have been detected on inverter–fed machines rated as low as 440 V [2]. These discharges gradually erode the thin polymeric film insulation eventually leads to the breakdown. The purpose of this study is to present results from ac 60 Hz breakdown voltage tests of polyimide insulated machine winding for obtaining the lifetime characteristics under normal operating condition.

Modern electrical machines must be designed as rugged and flexible. The use of power electronics devices cause voltage spikes and introduce harmonics that electrically degrade the insulation of the windings in the machine. High frequency power electronic

driver circuit also increases the operating temperature, which affect the aging and breakdown properties of the machine winding insulation. Knowledge of the machine winding insulation electrical degradation process is of critical importance in order to mitigate costs that include redundancy and the time involved to repair coil windings in the electrical machine. It is necessary to evaluate the lifetime characteristics of machine-winding insulation accelerated aged by high frequency pulse voltage than conventional 60 Hz ac and dc voltage [3-7].

Electrical insulation of inverter-fed motors is exposed to repetitive, short-rise time pulse voltage. Enhancements in modern power electronic devices such as the Insulated Gate Bipolar Transistor (IGBT) result in short rise time pulse voltage which is in the order of tens of nanoseconds. The short-rise time voltage introduces problems regarding the design and material selection of the electrical insulation in motor windings. Even for other types of voltage waveforms in a power system, dc or ac 50 Hz to 400 Hz, power electronics devices will be used. Use of the power electronics introduces the short-rise time transient over-voltages in an electrical insulation system, resulting in the accelerated aging of the electrical insulation. Over-voltages from the impulse can exceed the partial discharge inception voltage for the electrical insulation of the motor winding. The study of partial discharge and breakdown voltage is important for determination of electrical insulation reliability for inverter-fed motors [8-11].

1.2 Program of Study

In practical applications, the motor winding insulations are subjected to various electrical and thermal stresses. The insulation must be evaluated under simulated service conditions in order to identify the possible factors that are affecting the condition of the insulation. This evaluation is done by conducting accelerated aging that combine electrical and thermal stresses at various voltage waveforms (60 Hz ac and pulse voltage) and temperatures.

The work is performed to find an empirical electrical-thermal model to estimate the lifetime if NEMA 16-C (polyimide insulation) is exposed to multi-stress service conditions, which includes 60 Hz ac voltage and elevated temperatures. The effect of partial discharge activity is also taken into consideration at the higher voltage. In most application cases, there is not an industrial recognized standard for insulation testing of machine winding insulation. It is common to subject standardized twisted pairs to different types of electric stress while being subjected to higher temperatures.

In addition, the application of high frequency pulse voltage results in rise in the temperature of wire causes by joule heat, and falling of voltage endurance [12]. The desire frequency of square pulse voltage for an electrical machine is dependent on design requirement issues such as the material properties, thermal restrictions, and high frequency electromagnetic interference. Common electrical insulation testing frequencies for square pulse voltages are in the range of 10 kHz to 40 kHz, in order to simulate the high frequency over-voltages appearing due to the power electronic devices. Therefore it

is necessary to perform accelerated aging on machine winding insulation with high frequency pulse voltage in addition to 60 Hz ac voltage.

Modern insulation materials are designed to withstand degradation caused by partial discharges and to operate at higher temperatures. Thus, parameters for accelerated aging should include pulse voltage magnitude determined from partial discharge inception voltage. Temperature classes of winding insulation are defined in recent NEMA MW 1000 standard such as thermal class 155 (155ºC) [37].

Four different types of insulation material are chosen for this study. All selected machine winding insulations are 14 AWG heavy build insulation with 43μm thickness. The material types of insulations use in the study are as follow:

a) NEMA MW 35-C

b) NEMA MW 80-C

c) NEMA MW-16-C.

d) NEMA MW-73C

Partial discharge inception/extinction voltage and breakdown voltage measurements are performed on all samples after accelerated aging with high-frequency pulse voltage and temperature. These measurements are also performed for new samples with no accelerated aging.

This thesis presents the research work done in the High Voltage Laboratory where the electrical degradation study of magnet wire is studied under both 60 Hz ac and pulse voltage application. The lifetime characteristic of the NEMA MW 16-C is obtained at variable voltage, and temperature condition for 60 Hz ac voltage. Similarly, remaining

breakdown strength and partial discharge are measured for four different machine winding insulation accelerated aged by high frequency pulse voltage and high temperature.

1.3 Thesis Organization

The thesis is organized as follows. Chapter II discusses mainly the advent of adjustable speed drive (ASD) and possible causes of insulation failure in inverter fed motors. The chapter also reviews the research work done in the past to find out the possible causes of a premature breakdown of machine winding insulation supplied with the ASD. Chapter III presents the Weibull distribution used for the statistical analysis of machine winding insulation and common lifetime models. Chapter IV presents the physical phenomena of partial discharge with its measurement techniques. The common machine winding insulations with detailed information of tested insulations are discussed in chapter V. Chapter VI focuses on the experimental setup required to carry out the research work, both with high frequency pulse voltage and 60 Hz ac voltage. The experimental results are presented in chapter VII. Finally, chapter VII concludes the research work with possible future work to be performed in the High Voltage Laboratory.

CHAPTER II

LITERATURE REVIEW

2.1 Adjustable Speed Drive in Motor

Motors absorb about 70% of the electrical energy used in North America [13]. The induction motor is the most commonly used motor in the low and medium power range. During the development period, the induction motors are limited to deliver constant and non-adjustable speed. Furthermore, many applications of motors do not require running them at maximum power output. There is an increasing trend to accept variable speed technology in order to save the energy associated with running a motor at a lower speed. With an emphasis on energy conservation and lower cost, the use of a higher performance adjustable speed drive has rapidly grown up [14].

Generally, ac induction motors use pulse width modulation (PWM) – type inverters that have utilized insulated gate bipolar transistor (IGBT) technology since 1994 [13]. IGBT technology can provide very fast rise time surges in the range of a few tens of nanosecond to microseconds. The wire insulation of inverter-fed motors experiences a pulse voltage with significant harmonics and transients instead of conventional sinusoidal voltage.

Pulse width modulation, such as the example shown in the Figure 2.1 is easily converted to a lower frequency waveform with a simple low-pass filtering technique. The

parameters of the PWM pulse shape are shown in Figure 2.2

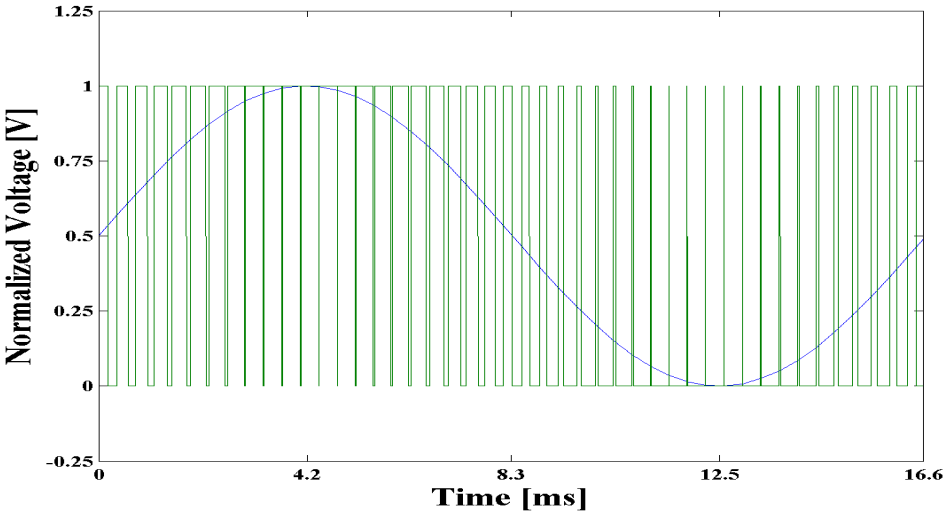

Figure 2.1 Example of using PWM to modulate a 60 Hz sinusoidal waveform

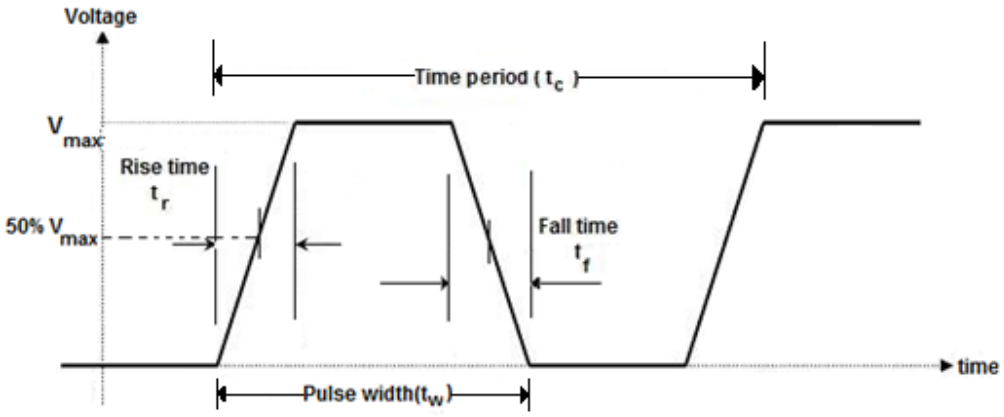

Figure 2.2 Parameters of square voltage: rise time, fall time, pulse width, and time period

Improvements in power electronic drive technology can provide advantages in terms of switching loss reduction and improved stability of motor torque. Unfortunately,

the use of the PWM converter under certain circumstances can lead to a premature failure of the winding insulation [15 and 16].

2.2 Causes of Insulation Failure in Motor with Adjustable Speed Drive

The main reason for the insulation failures in motors with adjustable speed drive are summarized below.

2.2.1 Electrical Aging Mechanism

Electrical aging mechanism is mainly related to voltage waveform and partial discharge activity. In a conventional 60 Hz motors rated up to 575 V, the maximum possible voltage stress across two layer of turn insulation could be low enough to deteriorate the insulation [17]. In contrast with 60 Hz sinusoidal voltage, the inverter-fed motors may cause voltage aging. Moreover, when entering into motor windings, the fast rising surges distribute unevenly along coil, and the most of the surge voltage is distributed between the first and second turns. These surges cause the voltage in the turn to be higher than partial discharge inception voltage (PDIV); even when low voltage is applied to the motor. The voltage between turns in the first coil may be 50% of the applied impulse voltage if the rise time is as short as 100 ns [17]. When the surge exceeds PDIV, partial discharge ignites and continues with a high repetition rate, which finally leads to insulation breakdown.

The presence of small air gaps between turns and between turn and ground resulted in higher electrical stress than Paschen minimum breakdown voltage (about 3kV/mm). Use of the partial discharge measurement technique is increased to evaluate

the reliability of rotating machines insulation. However, the effect on the partial discharge behavior of the resulting voltage distortion in inverter-fed motors is not satisfactorily explained yet. Hudon [18] observed in his study that a surface charge resulting from aging was proportional to the rise time of the steep pulse, but not to partial discharge activity. It is observed that aging under high frequency pulses occurs even in the absence of partial discharges activity. Furthermore, synergetic effects between injected space charge, temperature, and partial discharge activity complicates the understanding of these processes and require extensive research [19].

2.2.2 Thermal Aging Mechanism

When the insulation is under stress, heat is continuously generated within the dielectric due to conduction currents and dielectric losses due to polarization. At 60 Hz, dielectric losses cause heating of the insulating materials. The heat generated per unit volume and unit time is:

$$P = \varepsilon_0 \varepsilon' tan\delta \omega E^2 \tag{2.1}$$

where E is the electric stress, $tan\delta$ is dissipation factor, ε_0 is the permittivity of vacuum, and ε' is the relative permittivity of insulating material. At low frequency the losses usually increases with temperature.

At dc voltage, the heat generated per unit volume and time is:

$$P = \sigma E^2 \tag{2.2}$$

where σ is conductivity of the insulating material. The power loss is also increases with temperature.

The generated heat increases with the applied voltage. In general, the conductivity (σ) and dissipation factor ($tan\delta$) increases with temperature. A condition of instability is reached when the rate of heating exceeds the rate of cooling. At a certain voltage, the generated heat is higher than the dissipated heat at all temperatures; the temperature increases steadily and the material is destroyed [20].

Premature failure in inverter-fed motors can be attributed to accelerated aging due to insulation heating by dielectric and ohmic loss. Failure of insulation in a conventional motor is most often the result of deterioration due to long term thermal aging [21]. If the machine winding temperature is high enough, then thermal and chemical reactions take place and gradually reduce the electrical and mechanical properties of the insulation bonding material.

The high frequency pulse voltage appears in the machine winding due to the use of PWM converters. These surges cause capacitive current through the insulation to increase, increasing the power consumed within the dielectric and thus increasing the insulation temperature [15]. Consequently, PWM converters cause the machine winding temperature to be higher than for a conventional motor while all other things are equal, and therefore thermally age the insulation faster.

2.3 Previous Research

In past decades, the research was done on designing an aging model of insulation that were subjected to multi-stress such as electrical stress combined with thermal and mechanical stress [22], but only limited work was done to find out the effect of the high frequency pulse type of electrical stress.

In the early 80's, before the use of a current source inverter, the only concern for the turn-to-turn insulation capabilities of the motor coils was the switching surge disturbance in a power system [23]. However, extensive use of power electronic driver circuit enhanced the generation of fast rising pulse voltage. In fact, the fast rising high frequency pulses do not show an immediate response, but the long time exposure will lead to the premature failure of the insulation. Filter circuit may be employed to reduce the effect of fast rising pulse voltage. However, higher costs associated with filters rule out their use, especially for low voltage and low power motors.

R. H. Rehder, 1993, studied the increase in withstand capacity of partial discharge resistant enamel winding with surge voltage application [24]. In the study, the sample was subjected to 60 surges per second with an applied voltage of 8 kV and rate of rise of 0.2μs. This voltage level is much higher than a low voltage, inverter-fed motor would experience. Kaufhold [25] thoroughly studied the failure mechanism of low voltage inter-turn insulation as a consequence of partial discharge and explained the variation of partial discharge phenomenon with insulation design, temperature, and the applied voltage. He did not discuss the effects of pulse frequency and rise time. Skibinski et al. [26] developed the test method to determine the dielectric withstand levels of an ac motor in order to co-relate this withstand level to IGBT drive induced surge voltage. This model also presented partial discharge due to reflected voltage stress as a possible motor failure mechanism.

M. Yin [27] studied the effect of critical factors, which characterize the power inverters (voltage, frequency, rate of rise, duty cycle) to understand the premature failure

of wire insulation. The frequency can be varied up to 20 kHz and the rate of rise up to 67 kV/μsec. The author showed that failure of magnet wire under repetitive pulses was the combined effect of partial discharge, dielectric heating, and space charge formation. The insulation must have partial discharge resistant coating, and charge dissipation coating to eliminate the space charge built up during fast rise time pulses. The insulation must have high thermal stability to prevent damage caused by dielectric heating resulting from pulses with fast rise time and high frequency [27]. D. Fabiani [28] and group showed that high frequency sinusoidal voltage reduced the life of magnet wire both in presence and absence of partial discharge, but the reduction became prominent in partial discharge regime.

A number of research are underway to mitigate the partial discharge problem with the introduction of insulation materials that are resistant to partial discharge by increasing insulation thickness and/or by improving resin impregnation processes [16, 29, and 30].

CHAPTER III

STATISTICAL ANALYSIS ON INSULATION DEGRADATION

3.1 Weibull Distribution

Statistical methods must be used to describe and predict the breakdown voltage mechanism in insulation system study. Weibull distribution is a life-distribution model used for the time-to-failure model of electrical insulation. The Weibull distribution is preferred for its flexibility in taking many shapes for various values of the shape parameter, and thus it assists in modeling a wide variety of life data [31].

There are three types of Weibull probability density functions, depending upon the number of parameters that defines the given probability density function (*pfd*). The three parameters are defined as scale parameter (α), shape parameter (β), and location parameter (γ). Generally, the normal (Gaussian) distribution gives a suitable approximation of the mean value. So for measuring the breakdown strength of insulation materials having both high and low probabilities, the Weibull distribution gives a better approximation than the Normal distribution.

In Weibull distribution, three parameter need to be chosen in order to adjust to distribution of the measured results. It is difficult to find a definite solution with this distribution since several parameter combinations can give the same alignment. Due to

the same alignment, two-parameter Weibull distribution is commonly used which constitutes the scale parameter (α) and shape parameter (β). At each stress level the times to breakdown is determined using the two-parameter Weibull distribution. The cumulative probability of such a distribution is given as [31]:

$$F(t) = 1 - e^{\left[-\left(\frac{t}{\alpha}\right)^{\beta}\right]} \tag{3-1}$$

where $F(t) = \frac{(i-0.3)}{(n+0.4)}$ is the percentile of samples failed after a time t, α is the 63.2% nominal life time, β is the shape or variance parameter, i is the failure order number, and n is the total sample size. The reliability function of a distribution is simply one minus the cumulative probability distribution. The reliability function of the two-parameter Weibull distribution is given by

$$R(t) = e^{\left[-\left(\frac{t}{\alpha}\right)^{\beta}\right]} \tag{3-2}$$

The effect of β on the cumulative distribution function (cdf) and Reliability function are shown in Figure 3.1 and Figure 3.2 respectively.

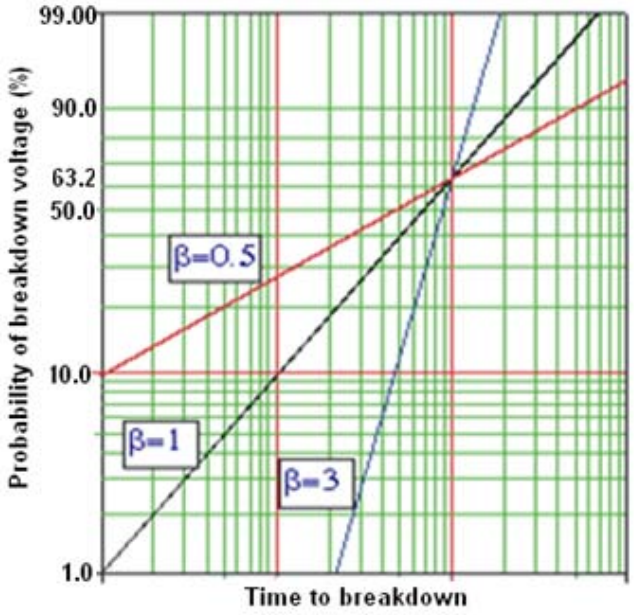

Figure 3.1 Effects of β on the *cdf* on a Weibull probability plot with a fixed value of α [31]

The figure shows that for same value of scale parameter (α), the slope of the line for different value of β is different. Due to this reason, this parameter is referred to as the slope parameter. The value of β is equal to the slope of the regressed line in a probability plot. Different value of the shape parameter can have marked effects on the behavior of the distribution. Figure 3.2 shows the effects of these varied values of β on the reliability plot.

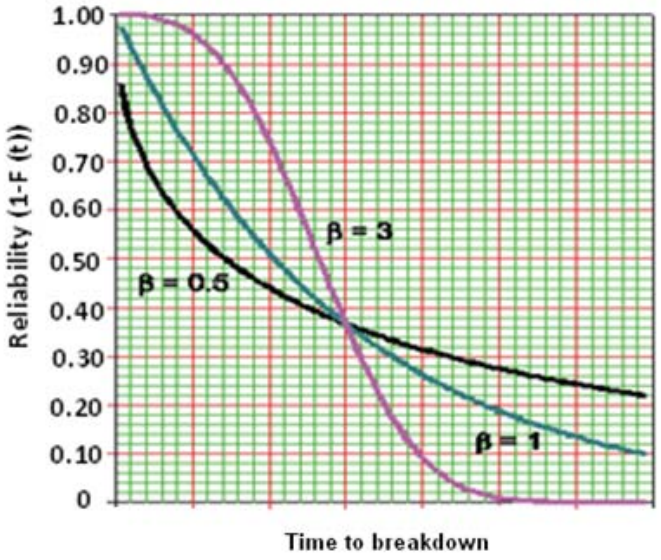

Figure 3.2 The effect of values of β on the Weibull reliability plot [31]

The conclusion drawn from the above figure can be summarized as [31];

- Reliability(*R (T)*) decreases sharply and monotonically for 0< β<1 and is convex.
- For β = 1, *R (T)* decreases monotonically but less sharply than the first case.
- For β>1, R *(T)* decreases as T increases.

3.2 Lifetime Models

As discussed in the previous chapter, failure of machine winding insulation is caused by combined electrical and thermal stress. When new insulation is used in any power apparatus, it is imperative to determine the operating electrical and thermal stress that can be applied in order to obtain a sufficiently long service life period. Usually the service life of 30 years is considered reasonable for a power apparatus [32]. Depending on the equipment use and conditions, the nature of the insulation is particularly designed to meet a variety of needs. To determine the lifetime model of any insulation prior to

installation, accelerated aging needs to be performed which is usually above the required operating stress level. The long-term tests at realistic working stress are not possible due to the time constraints. The lifetime is measured as a function of the stress and the expected lifetime at service condition is found by extrapolation. This method, however, raises a number of problems;

- The "lifetime" has no precise definition and
- The rate of degradation varies with the stress parameter in an unknown way, and still the subject of study.

It is therefore common to perform accelerated aging with one or a few dominant stress parameters, while the others are kept near operating stress. Single stress and multi-stress life models are mainly to estimate the lifetime model of the insulation.

3.2.1 Single Stress Life Models

Various experiments have been performed and models proposed to predict life under singular stresses. Of these, the most frequently used models are the inverse power and the exponential model under electrical stress only. Correspondingly, for thermal stress only, the Arrhenius relationship of exponential character is used extensively.

3.2.1.1 Electrical Stress

Electrical life models mathematically describe the aging mechanism in a solid dielectric insulation that experiences an electric stress. These models do not represent the exact aging mechanism occurring in the insulation. They only relate the rate of insulation

aging as power or exponential decay. The electrical aging models can be divided into two groups; inverse power model and exponential model.

3.2.1.1.1 Inverse Power Model

The inverse power model has been used frequently to estimate lifetimes of insulating materials under voltage stress. This model can be expressed as;

$$L(V) = K\,V^{-n} \tag{3-3}$$

where *L(V)* is the time to breakdown, usually taken as the Weibull scale parameter (α) at 63.2% probability of breakdown, *V* is the applied voltage, and *K* and *n* are constants which depend upon the material and aging conditions. By plotting the graphs with the time to breakdown for corresponding voltage stress in logarithm plot, a straight line is obtained, which determines the constant parameters [33].

3.2.1.1.2 Exponential Model

An alternative, exponential life model is given by;

$$L(V) = C.\exp(-DV) \tag{3-4}$$

Where:*C* and *D* are constants of the material and *V* is the value of applied voltage. The exponential model is valid only if the data represented on a logarithm fits the straight line [33].

3.2.1.2 Thermal Stress

The basis of a thermal aging model is well-known as Arrhenius chemical reaction rate model. The Arrhenius model predicts failure acceleration due to an increase in temperature. The model is one of the earliest and most successful acceleration models

that predict how time-to-failure varies with temperature [33]. This empirically-based model takes the form;

$$L(t) = A\ exp\frac{B}{T} \tag{3-5}$$

where A (1/time) is a material constant with respect to temperature, $B = \frac{Q}{R}$; Q (J/mole) is the activation energy, R = 8.3 (J/K .mole) is a gas constant, and T (ºK) is the absolute temperature.

3.2.2 Multi-stress Life Models

Aging under multi-stress is an area that has recently generated considerable interest. Simultaneous electrical and thermal stresses have been most commonly investigated as the presence of these two stresses is almost unavoidable in most applications. For multiple stresses, particularly for electrical and thermal stresses acting simultaneously, several models have been proposed. The models are based on combined thermal and electrical stress by Simoni and Ramu [22], the exponential model by Fallou [22], and probabilistic model by Montanari [34]. The probabilistic life model of combined electrical and thermal stresses relates the failure probability to insulation lifetime. It is based on substituting the scale parameter in the Weibull distribution with the life using the inverse power law.

In a multi-stress situation, the parameter A in Eq.(3-5) will be the function of all the other applied stresses, and assuming n in Eq.(3-3) to be independent of temperature, activation energy (Q) to be independent of the applied voltage, combining Eqn.(3-3), and Eqn.(3.5), we have [32]

$$L(t,V) = W.\exp\left(\frac{Q}{RT}\right).V^{-n} \tag{3-6}$$

where W is the new material constant under multi stress conditions. Thus plotting the logarithm of the lifetime as a function of inverse of temperature (ºK), a straight line with the electrical stress as a parameter is obtained which is given as:

$$lnL(t,V) = lnW - nV + \left(\frac{Q}{R}\right).\left(\frac{1}{T}\right) \tag{3-7}$$

It is well-known that partial discharges in insulating materials may cause a gradual deterioration until insulation punctures and electric breakdown occurs. Partial discharge activity is found to be responsible for driving the aging phenomena. It is the fact that different aging processes take place at different stress conditions that makes it difficult to predict the exact lifetime during the service condition. Although, much work has been done to find a relation between time to breakdown and partial discharge magnitude, no general relation has been established [32]. It has been found that internal discharges become more detrimental at higher electric stress. This effect is caused by an increasing energy ΔW evolved per discharge, which is increasing with effective extinction voltage, V_e and apparent charge, q_a according to:

$$\Delta W = \sqrt{2}.V_e\ q_a \tag{3-8}$$

In addition, the effect of increasing the applied voltage is usually to increase both the number of partial discharges and the magnitude of the apparent charge. The rate of aging is strongly enhanced by partial discharge activity and the mechanism of aging becomes very different from that of voltage aging without partial discharges [32].

3.2.3 Multi-stress Life Model with High Frequency Pulse Voltage

In the previous aging models, the multi-stress life models cannot have high frequency pulse voltage as a electrical stress. The work was done at Mississippi State University using high frequency square pulse voltage as an electrical stress to obtain the lifetime model of magnet wire insulation [3-7]. S. Grzybowski et al. deduced the frequency-electrical-thermal life model [3] based on the application of high frequency pulse voltage. The effect of frequency on the pulse voltage has been incorporated in the equation given below;

$$L(V,T,f) = K\, f^{\left(m1+\frac{m2}{V}\right)}\, exp\left(\frac{A}{V}+\frac{B}{T}\right) \tag{3-9}$$

where L is the lifetime in hours at 63.2% probability, V is the voltage in Volts, T is the temperature in Kelvin, and f is the pulse voltage frequency in Hz. The parameter K, A, B, m_1, and m_2 are constants determined using experimental data.

CHAPTER IV

PARTIAL DISCHARGE: LITERATURE REVIEW

4.1 Definition

In practice, it is very difficult to manufacture solid insulation in such a way that it is completely free of gas inclusions. During casting, extrusion, and impregnations gas-filled cavities are easily formed. Such cavities can be formed because of poor contact between electrodes and insulation. The main reason for the relatively low strength of solid insulation is the presence of air voids either in the material or at the surface when insulation is subjected for long periods to electrical stresses. Although much improvement has been done in the technology of impregnation, the presence of single discharging voids still create problem which eventually leads to much anticipated breakdown. Even without the presence of initial voids, chemical reactions and thermal or mechanic shock may produce the voids necessary for electrical failure by partial discharge mechanism [35].

According to IEC standard 60270 [36], partial discharge is a localized electrical discharge that only partially bridge the insulation between conductors and which can or cannot occur adjacent to a conductor. Over the years, partial discharge test has become one of the most important tests for insulation quality assessment. Partial discharge occurs in micro cavities when present in the insulation of electrical machines.

Partial discharge activity is the most prominent indicator of insulation deterioration assessment. It is a widely used non-destructive method to evaluate the reliability of insulation conditions [8-11]. Common machine winding insulation materials like polyethylene, polyester, polyimide, and polyurethane have very high dielectric strength. Conversely, air has a relatively low dielectric strength. As there is small gap left between turn and turn insulation and between turn and ground, electrical breakdown in air causes an extremely brief electric current to flow through the air cavity. The measurement of partial discharge is, in fact, the measurement of these breakdown currents. The electrical insulation of machines is susceptible to:

- Thermal stresses
- Chemical attack
- Abrasion due to excessive coil movement

In all cases, these stresses will weaken the bonding properties of the insulation that coat the windings. There are three type of partial discharge activity present depending upon their location of occurrences and they are;

- Internal discharge that occurs in voids or cavities.
- Surface discharge that occurs in surface of the insulation.
- External discharge that occurs in strong non homogenous field around edge.

4.2 Partial Discharge: Physical Phenomena

There are various ways to measure the partial discharge activity. Strong partial discharge may be audible or visible, but small discharges in cavities cannot be observed

directly. The partial discharge activity produces electrical pulses, ultra high frequency (UHF) waves, acoustic emissions (AE), local heating, and chemical reactions.

In order to investigate the possibilities of an electrical measuring method, it is necessary to analyze the physical phenomena behind partial discharge. Figure 4.1(a) shows the cross-section of solid dielectrics of thickness *d* containing the cavity of thickness *t*. If an ac voltage is applied to the electrodes, the equivalent circuit is that shown in part (b). The corresponding diagram represents the capacitance C_c of the cavity and the capacitance C_b of the dielectrics in series with the cavity. The capacitance C_a represents the rest of the dielectrics.

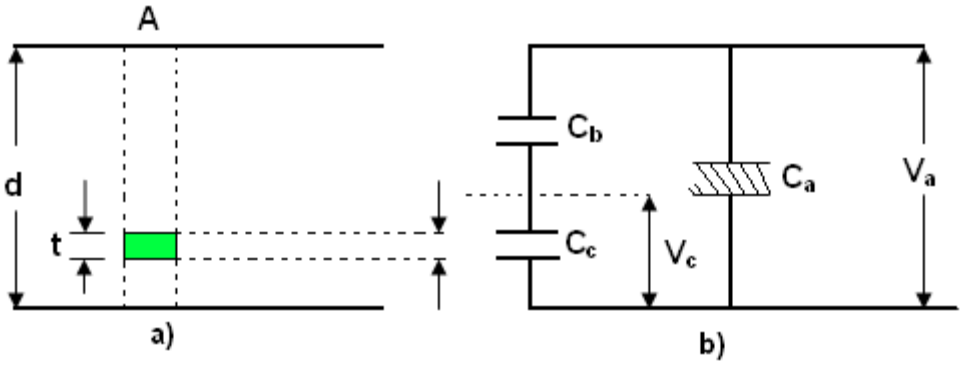

Figure 4.1 Electrical discharges in cavity and its equivalent circuit [20]

Assuming that the gas filled cavity breakdown stress is E_{cb}, and according to the configuration model [20 and 35];

$$C_b = \frac{o\ rA}{d-t} \tag{4-1}$$

$$C_c = \frac{o\ A}{t} \tag{4-2}$$

The voltage across the cavity is

$$V_c = \frac{C_b}{C_c+C_b} V_a = \frac{V_a}{1+\frac{1}{\varepsilon_r}\left(\frac{d}{t}-1\right)} \tag{4-3}$$

Therefore the voltage across the dielectric, which initiates discharge in the cavity, is given by

$$V_{ai} = E_{cb} t \left\{1 + \frac{1}{r}\left(\frac{d}{t} - 1\right)\right\} \tag{4-4}$$

In a spherical gas-filled cavity, which constitutes only a small portion of the insulation thickness, the maximum electric stress is

$$E_c = \frac{3\varepsilon_r E}{rc+2\varepsilon_r} = \frac{3E}{2} \tag{4-5}$$

for $\varepsilon_r \gg \varepsilon_{rc}$, where E is stress in the solid dielectric in the absence of cavities. According to Eq. 4.5, the stress in the cavity is higher than in the solid insulation. The normal operating electric stress in high voltage equipment is usually high, and there is a risk of discharge within a cavity without breakdown of solid insulation.

The sequence of breakdown under sinusoidal alternating voltage is presented in Figure 4.2.

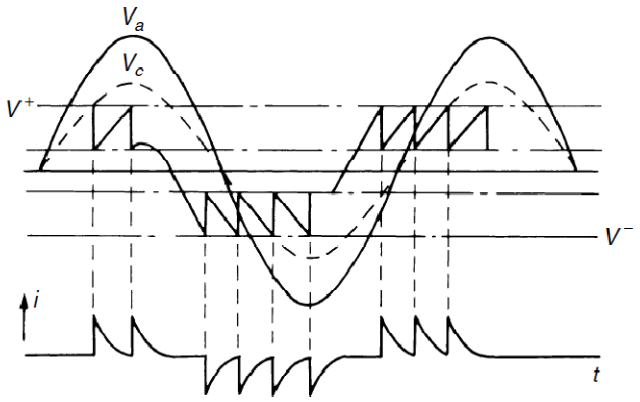

Figure 4.2 Sequence of cavity breakdown under alternating voltages [20]

When sinusoidal voltage V_a is applied and voltage across the gap reaches V+, the cavity may break down. When V_c reaches the value V+, a discharge occurs, the voltage V_c collapses, and the gap extinguishes. The voltage in the gap starts to increase when it reaches V^+, and then a new discharge occurs. Several discharges may be observed during the positive half-cycle of the applied voltage. If the applied voltage is higher than the minimum required for the breakdown, a further rise in voltage overcomes the decrease in field, due to the collected charge, and a further pulsed discharge occurs. In the negative half- cycle, accumulated charge from the past half-cycle adds to the applied voltage, and breakdown may even occur during the zero crossings. In the negative half-cycle, the cavity discharges as the voltage across it reaches V^-. The measurement of partial discharge is in fact measurement of these discharge pulses [20 and 35].

4.3 Partial Discharge Measurement

The necessary measurements needed for the partial discharge analysis in the test results are as follow;

4.3.1 Partial Discharge Inception Voltage (PDIV)

In order to measure partial discharge inception voltage, voltage below the expected inception voltage is applied to the test object and is gradually increased until discharges reach, or exceed, a specified low magnitude [36]. The partial discharge inception voltage is marked by the appearance of the partial discharge pulses, which are visible on the partial discharge detector. The partial discharge inception voltage depends

on the rate of rise of the applied voltage. In order to have a uniform measurement for different samples, the voltage is increased at the rate of 20V/sec.

4.3.2 Partial Discharge Extinction Voltage (PDEV)

When the sample for the test is connected to the partial discharge detector circuit, the voltage is increased at the rate of 20 V/sec to obtain the required partial discharge inception voltage. The voltage is then increased to a specified voltage level and then gradually reduced to a value at which the discharge becomes less than the same specified magnitude. The test voltage at this discharge limit is the partial discharge extinction voltage [36]. The value of PDEV is affected by the amplitude and time of voltage application and also by the rate of decrease of voltage.

4.3.3 Three-Dimensional Analysis of Partial Discharge

The measurement of partial discharge activity is shown in the three- dimensional plot so that aging phenomena can be comprehensively observed during aging conditions. The three-dimensional analysis constitutes the φ-q-n (φ: phase, q: partial discharge magnitude, n: partial discharge pulse count) pattern.

4.4 Partial Discharge Measurement System

There are two common systems for partial discharge measurements. Most circuits in use for partial discharge measurements are derived from one or other of the basic circuits, which is shown in Figure 4.3 and Figure 4.4

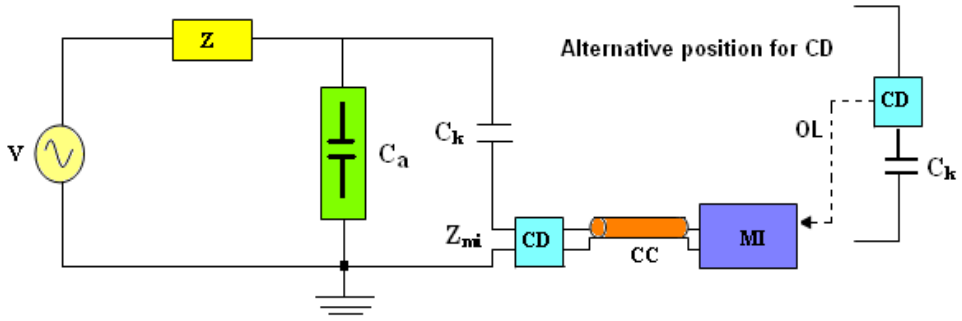

Figure 4.3 Coupling device CD in series with the coupling capacitor [36]

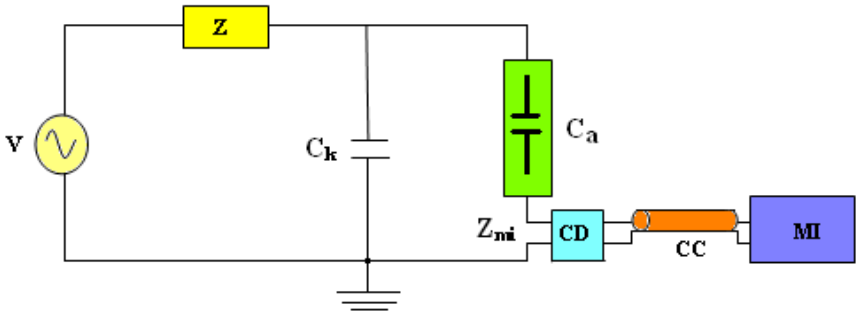

Figure 4.4 Coupling device CD in series with the test object [36]

Components:

V High-voltage supply

Z_{mi} Input impedance of measuring system

CC Connecting cable

C_a Test object

C_k Coupling capacitor

CD Coupling device

MI Measuring instrument

Z Filter

The description of the components is as follows;

- Capacitor, C_a, represents a test object.
- The Coupling capacitor, C_k , has a low inductance value and should have sufficiently low partial discharge values at the specified test voltage for the measurement of the specified partial discharge magnitude.
- A measuring system with its input impedance.
- A high-voltage supply, with a sufficiently low level of background noise.
- High-voltage connections, with a sufficiently low level of background noise.
- A filter in the high voltage side to reduce background noise from the power supply.

For the basic partial discharge test circuit shown in Figure 4.3, the coupling device of the measuring system can also be placed at the high-voltage terminal side. In the above case, the position of the coupling device with C_a and C_k need to be exchanged. The connection of the coupling device with the instruments is done with optical links. This configuration is necessary when the test object has grounded terminal [36]. The experimental setup for the partial discharge measurement system will be discussed in chapter VI.

CHAPTER V

MACHINE WINDING INSULATION

5.1 General Insulating Materials

Machine winding consists of a copper or aluminum conductor and a thin layer of insulation over the conductor. Table 5.1 represents the generally used insulation types and their corresponding thermal rating [37]. It can be observed that the most used insulation types are polyurethane, polyester, polyamideimide, and polyimide.

Table 5.1

Properties and requirement listing by thermal class, insulation, coating and form for film insulated round magnet wire [37]

Thermal Class	**Insulation, Covering and Form**	**NEMA Specification**
105	Polyamide	MW 6-C
105	Polyvinyl acetal	MW 15-A, MW 15-C
105	Polyvinyl acetal over coated with polyamide	MW 17-C
105 Solderable	Polyurethane	MW 2-C
105 Solderable	Polyurethane and self-bounding overcoat	MW 3-C
105 Solderable	Polyurethane overcoated with polyamide and self-bonding overcoat	MW 19-C
105	Polyvinyl acetal and self-bonding overcoat	MW 19-C
130 Solderable	Polyurethane overcoated with polyamide	MW 28-A, MW 28-C

Table 5.1 (continued)

130 Solderable	Polyurethane overcoated with polyamide and self-bonding overcoat	MW 135-C
155	Polyester	MW 5-C
155	Polyester (amide)(imide) overcoated with polyamide	MW 24-A, MW 24-C
155 Solderable	Polyester (imide)	MW 26-C
155 Solderable	Polyester (imide) overcoated with polyamide	MW 27-C
155 Solderable	Polyurethane	MW 79-C
155 Solderable	Polyurethane overcoated with polyamide	MW 80-A, MW 80-C
155 Solderable	Polyurethane with self-bonding overcoat	MW 131-C
155 Solderable	Polyurethane overcoated with polyamide and self-bonding overcoat	MW 135-C
180	Polyester (amide)(imide) overcoated with polyamide	MW 76-A, MW 76-C
180	Polyester (amide)(imide) overcoated with polyamideimide and self-bonding overcoat	MW 102-A, MW 102-C
180 Solderable	Polyester (imide)	MW 77-C
180 Solderable	Polyester (imide) overcoated with polyamide	MW 78-C
180 Hermetic	Polyester (amide)(imide)	MW 72-C
180 Solderable	Polyurethane	Mw 82-C
180 Solderable	Polyurethane overcoated with Polyamide	MW 83-C
200	Polyester (amide)(imide) overcoated with polyamideimide	MW 35-C
200	Polyester (amide)(imide)	MW 74-C
200 Hermetic	Polyester (amide)(imide) overcoated with polyamideimide	MW 73-C
220	Polyester (amide)(imide) overcoated with polyamideimide	MW 35-A

Table 5.1 (continued)

220	Polyester (amide)(imide) overcoated with polyamideimide	MW 37-C
220	Polyester (amide)(imide)	MW 74-A
220 Hermetic	Polyester (amide)(imide) overcoated with polyamideimide	MW 73C, MW 73-A
220	Polyamideimide	MW 81-C
240 Hermetic	Polyimide	MW 16-C

**A-Aluminum*
**C-Copper*

5.2 Insulation Used for the Test

Four different types of insulation materials are chosen for this study among the available machine winding. All four machine windings are of 14 AWG size and heavy insulation build, with a thickness of 43.6 μm. Brief introductions of the selected insulations for the experiment are given below.

5.2.1 NEMA MW 35-C (IEC 60317-13)

This insulation consists of a polyester layer with a polyamideimide coating intended to resist partial discharge on the surface of the insulation. This machine winding is a two-part insulation consisting of a modified polyester basecoat with an amide-imide outer coating, with superior toughness and resistance to chemicals and moisture. It has higher thermal properties than polyester or polyester/nylon. The rated temperature of this insulation is 200ºC [38]. This insulation has been specifically designed for use in motors that may be subjected to higher voltage spikes present in inverter duty application. The general applications of the MW 35-C include;

- Fractional and Integral motors (hermetic and open)
- Automotive and hand tool armatures
- Dry type transformer
- Higher moisture applications

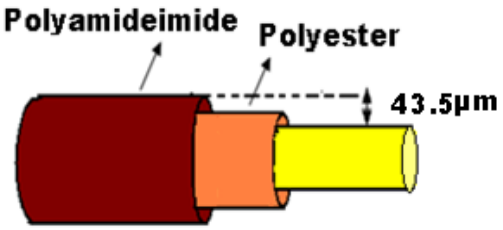

Figure 5.1 NEMA MW 35-C

5.2.2 NEMA MW 80-C (IEC 60317-21)

The next insulation tested is the NEMA MW 80-C (IEC 60317-21) wire insulation. This type of insulation consists of a polyurethane-nylon layer, with a rated temperature of 155ºC. Polyurethane can be soldered wire to wire and to terminals without prior removal of the wire insulation. Polyurethane-nylon combines the magnet wire insulation characteristics of polyurethane, with the advantages of a nylon topcoat which results in some loss of solderability. However, this insulation cannot be used in high current or high temperature applications, such as locked rotor condition. MW 80-C is generally used in encapsulated coils, relays, and yoke coils [38].

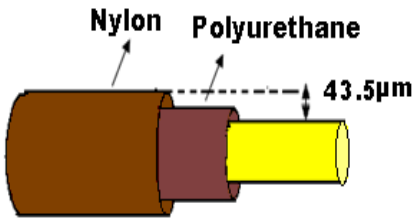

Figure 5.2 NEMA MW 80-C

5.2.3 NEMA MW 16-C (IEC 60317-46)

The third type of insulation tested is the NEMA MW 16-C (IEC 60317-46) wire insulation. Polyimide magnet wire is insulated with a smooth film of aromatic polyimide resins. It is Class 240°C insulation with exceptional resistance to chemical solvents and burnout [38]. Polyimide film is very resistant to high temperatures. This magnet wire is mainly used in products subjected to continuous high-operating temperatures and intermittent service overloads. Some typical applications of NEMA MW 16-C includes;

- Fractional and integral horsepower motors
- High temperature continuous duty coils and relays
- Hermetic and sealed units
- Heavy duty hand tool motors
- Encapsulated coils

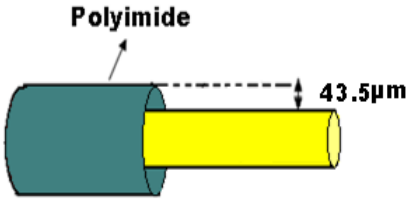

Figure 5.3 NEMA MW 16-C

5.2.4 NEMA MW 73-C (IEC 60317-25)

The last type of insulation class is NEMA MW 73-C (IEC 60317-25), class 220 ºC. It is a modified polyester basecoat with amide-imide topcoat, with superior toughness and resistance to chemicals and moisture. Its general applications are in fractional and integral horse power motors and dry type transformers [38].

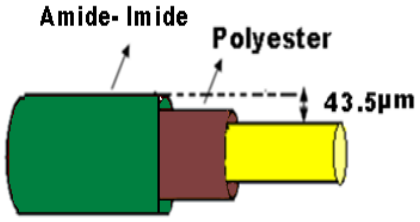

Figure 5.4 NEMA MW 73-C

CHAPTER VI

EXPERIMENTAL SETUP

6.1 Accelerating Aging with Pulse Voltage Application

A dielectric test system (DTS), as shown in Figure 6.1, is used to provide the accelerated aging environment for the electrical machine winding insulation samples. The DTS–1500 A is an integrated test system applicable for studying the failure mechanism of machine winding insulation by simulating the electrical and thermal stress under controlled and accelerated conditions. These stresses are primarily a characterization of inverter-fed motors. The DTS-1500A test system is designed to vary and monitor the electrical and thermal test parameters for up to five samples simultaneously. The system includes the following features;

- A 3,500 V magnitude pulse test system for accelerated degradation testing of twisted pair samples (the frequency of the square pulse voltage is set up to 40 kHz)
- Variable output voltage, frequency, Duty cycle, and temperature
- A convection air-circulating oven to facilitate testing at a controlled and elevated temperature (the temperatures are available from 40°C to 260°C)

Figure 6.1 The dielectric test system (DTS)

The control and monitoring of these parameters allow the user to study the insulation degradation and failure mechanism common to PWM applications. The DTS-1500A drastically reduces the test time from days per sample to minutes per sample when compared to the testing with the practical inverter. The reduced research time increases the probability of development and analysis of the new motor insulation. The system can simultaneously pulse five capacitive samples of 10 pF (a typical twisted pair) per sample in uni-polar mode. Typical output waveform is shown in Figure 6.2. The rise time of the applied pulse is approximately 50 ns.

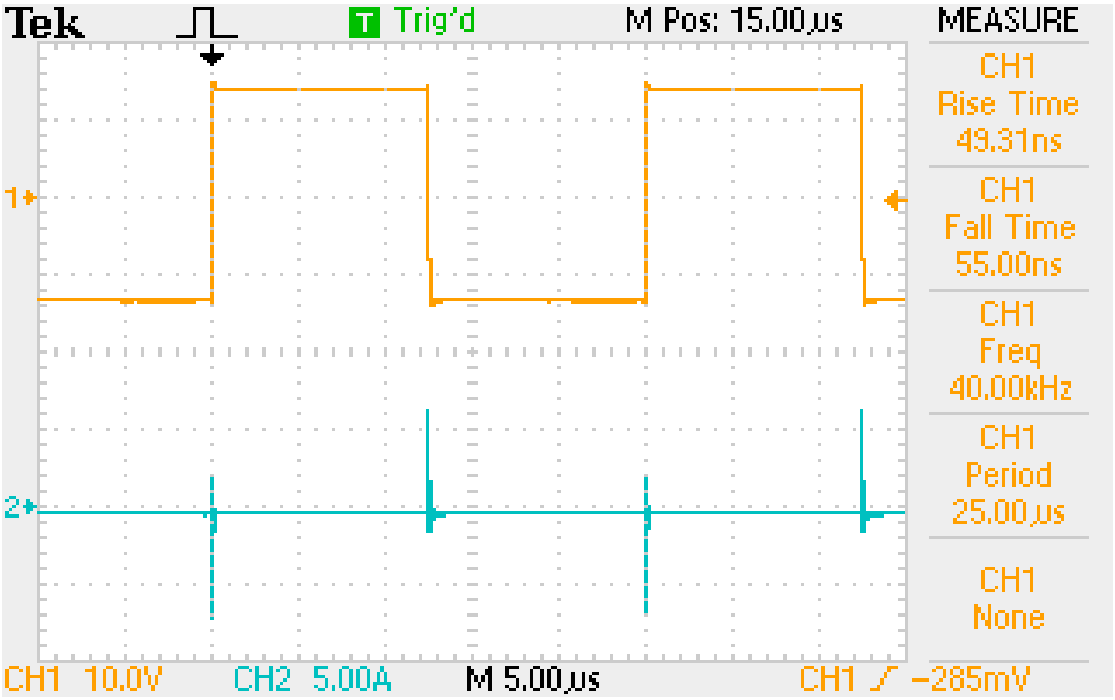

Figure 6.2 Typical voltage (top trace) and current (bottom trace) waveforms, driving a twisted pair

6.2 Sample Preparation

Although study of the electrical insulation system for a machine winding is important, it is a commonly accepted practice to study small twisted wire samples, as shown in Figure 6.3. According to the IEC 62068 standard [39], the application of simple waveforms, either bipolar or unipolar square pulse voltage, can be used for an aging insulation system or comparing their behavior with respect to a reference assessed insulation system.

Preparation of the twisted wire samples are specified by the NEMA standard for a number of twists at wire tension. A specimen of wire is formed into a "U" shape, and the two legs are twisted together the number of 360° rotations specified in Table 6.1 to form

an effective length of 4.75±0.25 inches (121 mm±6 mm). The total tension on the two legs and the total number of rotations is shown in Table 6.1 [37].

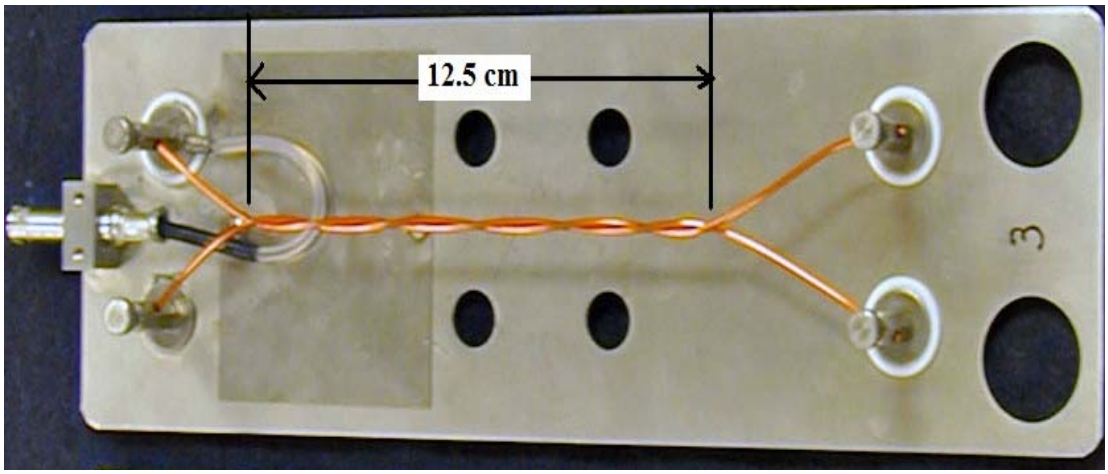

Figure 6.3 Twisted pair of sample place in the DTS tray

Table 6.1

Twisted pair method: Tensions and rotation [37]

AWG Size	Total Tension on Specimen (±2%)	Total Number of Rotation
8-9*	24 lb (107N)	3
10-11	24 lb (107N)	3
12-14	12 lb (53N)	4
15-17	6 lb (27N)	6
18-20	3 lb (13N)	8
21-23	1.5 lb (7N)	12
24-26	340 gm (3.3N)	16
27-29	170 gm (1.7N)	20
30-32	85 gm (0.8N)	25

Table 6.1 (continued)

33-35	40 gm (0.4N)	31
36-37	20 gm (0.2N)	36

The largest wire diameter that is possible in the DTS is a 14 AWG size round conductor. By the NEMA standard, no more than 4 full twists are allowed with a tension force of 12 pounds. Preparation of the samples is performed with a device that counts the number of twists and puts consistent tension on the wire during the twisting process. Figure 6.4 shows the dielectric twist fabricator used to prepare the samples according to the NEMA standard for a 14 AWG size round conductor. After preparation of the sample, insulation is removed from both ends of the wire for a solid electrical connection to the high voltage and ground terminal in the DTS.

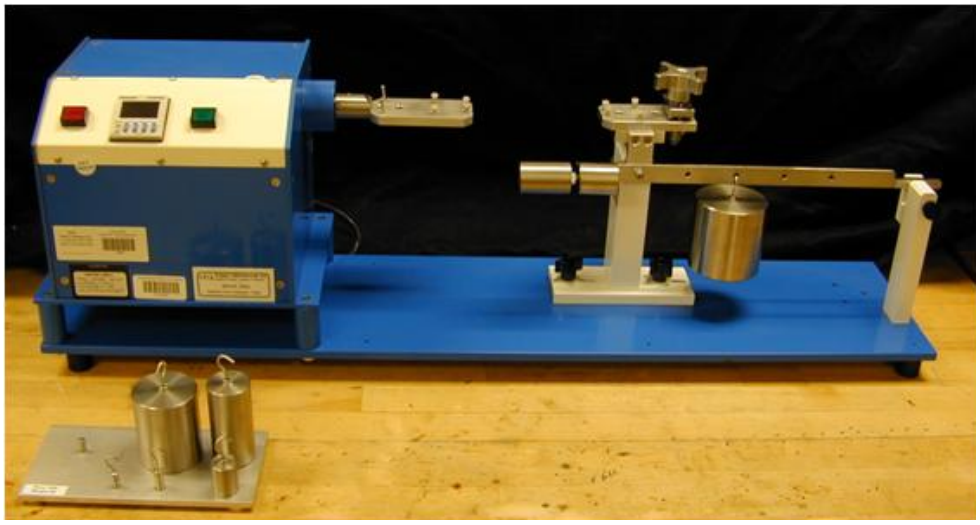

Figure 6.4 Dielectric twist fabricator

6.3 Partial Discharge Measurement

Partial discharge measurements are taken using the Hipotronics DDX-7000 digital partial discharge detector. The partial discharge is measured with the electrical method in which high frequency electrical disturbance develops in a localized area and propagates via the electrical circuit. The electrical method is useful when quantification of the partial discharge pulse is needed; for example, the analysis of magnitude, count, and phase of the pulse is possible with the electrical method of partial discharge detection. Figure 6.5 shows the DDX 7000 Detector used to measure the partial discharge.

Figure 6.5 DDX 7000 partial discharge detector

The Hipotronics DDX Detector can automate the entire partial discharge testing process, from voltage source control to calibration to test report generation. The DDX 7000 PD Detector has the following features;

- The mainframe, including PC, display, module rack, and power supplies
- 5 Modules: Amplifier, Display, Measure, Capture, and Calibrate

- Software
- Transient Filter Unit

The amplifier module amplifies and filters the partial discharge output before the signal is passed to the measure and capture modules. Partial discharge magnitude and the applied voltage are measured using the measure module. The capture module digitizes the partial discharge pulses for display and analysis. The experimental set up for the partial discharge measurement is shown in Figure 6.6.

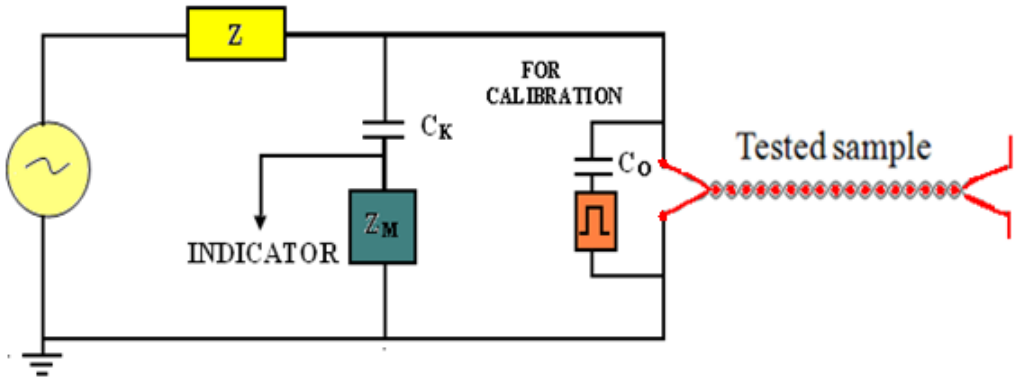

Figure 6.6 Partial discharge test system for twisted pair of sample

The figure presents the partial discharge test system used to test the twisted pair of sample. The components of the system are discussed according to IEC standard 60270. The calibrator generates the step voltage pulses of amplitude U_O with capacitor C_O in series. The calibrator produces repetitive charge, each with magnitude;

$$q_{o} = U_O C_O \tag{6-1}$$

Calibration pulses are generated as a series of unipolar voltage pulses characterized by a fast rise time [36]. During the measurement of partial discharge

activity, one terminal is connected to the high voltage, and the other terminal is connected to the ground for the twisted pair of samples, as shown in Figure 6.6. The test voltage is increased on the sample to achieve high electrical stress between twisted wires to simulate the electrical stress that exists between wires in the machine. During the measurements, one wire is energized, and the second wire is grounded.

The three-dimensional plot (φ-q-n pattern) is obtained to analyze the partial discharge's magnitude, phase, and pulse count comprehensively. The partial discharge measurement system consists of 40 kV ac sources and a 100 pF standard capacitor, which is connected to the DDX-7000.

6.4 Breakdown Voltage Measurement

Breakdown voltage is measured with the help of the NOVA 1401-LCT. Figure 6.7 shows the breakdown tester used in the experiment. The NOVA 1401-LCT performs the dielectric breakdown test on round, insulated magnet wire with heavy build insulation. The tester has a test voltage range of 0 to 30 kV. The rate of voltage rise is 20 to 500 volts per second. Voltage needs to be applied at the rise time of 250 V/sec to obtain the required breakdown.

Figure 6.7 Breakdown voltage tester

6.5: Accelerating Aging Conditions

Accelerated electrical degradation of the machine winding insulation materials is performed using square pulse voltage with a magnitude of 1300 V for NEMA MW 35-C and NEMA MW 80-C and 1350 V for NEMA MW 16-C and MW 73-C. The square pulse voltage frequency is 40 kHz and 20 kHz. The magnitude of the voltage is selected to limit partial discharge during the aging duration. In addition, 90% of the thermal rating temperature is selected as the aging test temperature. It is very important to select the correct voltage levels and temperatures during the accelerated electrical degradation process, as electrical-thermal degradation behavior of the winding insulation are important. The accelerating aging test conditions for the experiment are summarized in Table 6.2.

Table 6.2

Accelerated aging conditions

S.No	NEMA	IEC	Applied Pulse Voltage (V)	Frequency (kHz)	Temperature (°C)
1	MW 80-C	IEC 60317-21	1300	40	140
2	MW 35-C	IEC 60317-13	1300	40	180
3	MW 73-C	IEC 60317-25	1350	20	200
4	MW 16-C	IEC 60317-46	1350	20	216

6.6 Accelerating Aging with 60 Hz ac

The times to breakdowns are measured using samples of NEMA MW 16-C (IEC 60317-46) wire, rated for operation up to 240˚C. Figure 6.8 shows the experimental setup to obtain time to breakdown of NEMA MW 16-C insulation at various 60 Hz ac stress level.

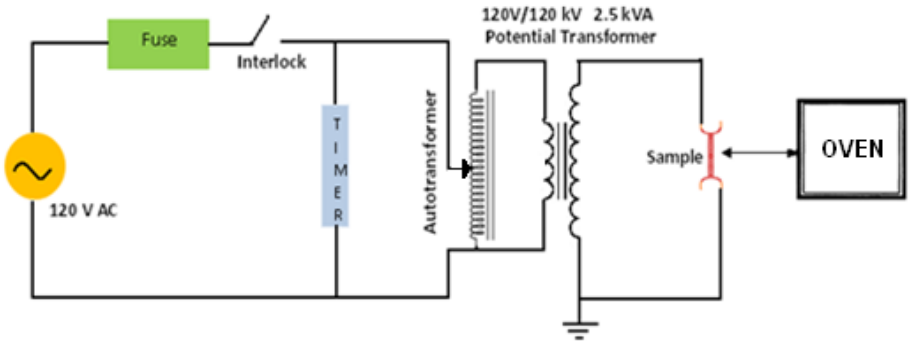

Figure 6.8 Setup diagram for ac voltage time to breakdown test

The ac test system consists of a 2.5 kVA, 120V/120 kV potential transformer, and a 0/120V autotransformer. The oven from Cenco Instrument provides the accelerated aging condition up to temperatures of 215°C. The twisted pair of samples is energized by the potential transformer until it breaks. When the sample is broken, the short circuit current flowing in the circuit breaks the fuse, which also stops the timer. Figure 6.9 shows the potential transformer and the oven used during the determination of time to breakdown for MW 16-C insulation.

Figure 6.9 Test setup for ac voltage time to breakdown test of NEMA MW 16-C

Two different types of test objects, shown in Figure 6.10, are used during the experiment. Figure 6.11(a) shows the twisted pair of sample tested with the schematic

diagram. Figure 6.11(b) presents the single terminated wire with a ground electrode of silver paint with the corresponding schematic arrangement.

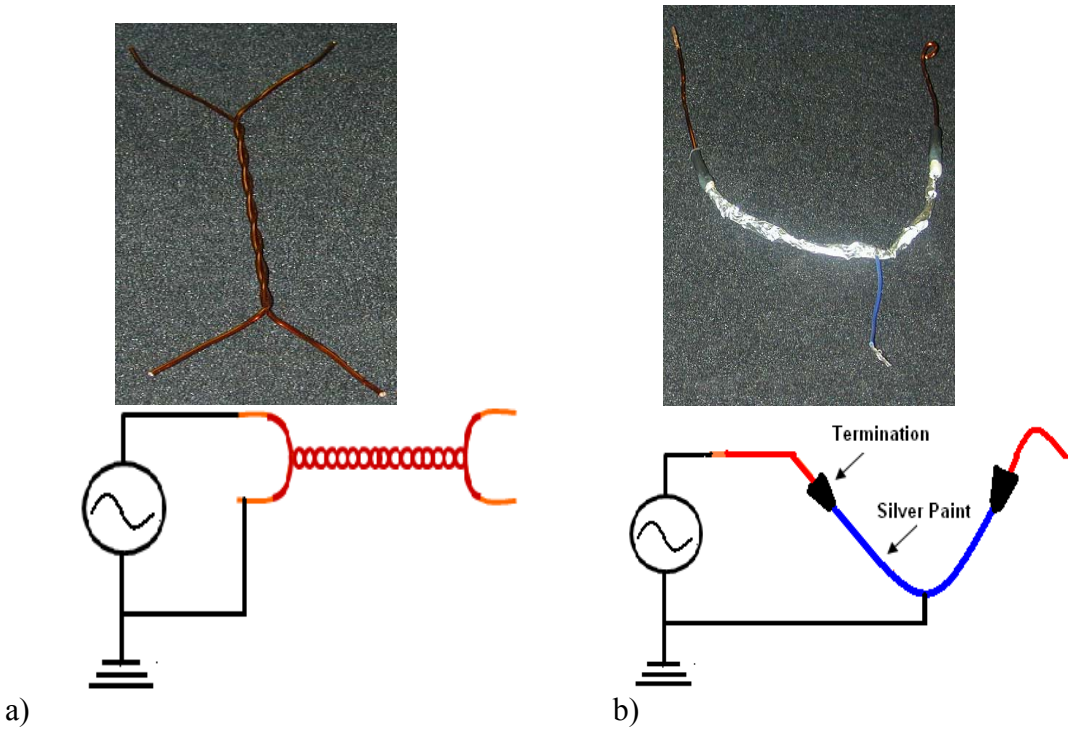

Figure 6.10 Test objects a) twisted pair b) single terminated wires with ground electrode of silver paint and Al-foil

The twisted pairs are made according to the NEMA standard, using 4 full twists to form a 125 mm long twisted section [37]. During aging, one side of the twisted pair is energized while the other is kept at ground potential. Thus, the applied ac voltage is equally distributed across the insulation of the two series connected wires.

It is observed that at an applied effective test voltage of about 0.65 kV, the E-field in the air-gap between the wire exceeded that of Paschen minimum (~3 kV/mm), and partial discharges inception occurred. In order to reduce the aging effect of such external

discharges, comparable breakdown tests are performed using single wires covered with 125 mm long silver painted ground electrodes.

Prior to aging, the partial discharge inception/extinction voltage and the apparent partial discharge level are measured versus test voltage, using the Hipotronics DDX-7000 digital partial discharge detector. The accelerated aging are conducted over the 60 Hz ac effective voltage range from 1.5 kV to 8 kV at room temperature of 23°C, and from 1.5 kV to 5 kV at 115°C and 215°C, using a minimum of four samples at each test condition. Breakdown voltage measurement using the single wire samples are performed at room temperature and at a test voltage of 2 kV only.

CHAPTER VII

TEST RESULTS

7.1 With 60 Hz ac Voltage

At each stress level, the times to breakdown are determined using the two parameter Weibull distribution. The cumulative probability of such a distribution is given as:

$$F(t) = 1 - e^{\left[-\left(\frac{t}{\alpha}\right)^{\beta}\right]} \tag{7-1}$$

where $F(t) = \frac{(i-0.3)}{(n+0.4)}$ is the percentile of samples failed after a time t, α is the 63.2% nominal life time, and β is the shape or variance parameter. The time to breakdown value is obtained for a minimum of four samples at the particular voltage level, ranging from 1.5 kV to 5 kV.

The Weibull plots in Figure 7.1 through Figure 7.5 show that in the case of twisted pairs, the shape factor β increases with test voltage, while being nearly invariant with respect to temperature. Such voltage dependence indicates a change in the physical aging process when the test voltage is increased from 1.5 kV to 5 kV. Table 7.1 represents time to breakdown (63.2% probability) values obtained from the Weibull distribution plot from 1.5 kV to 5kV for temperatures of 23°C, 115°C, and 215°C, respectively.

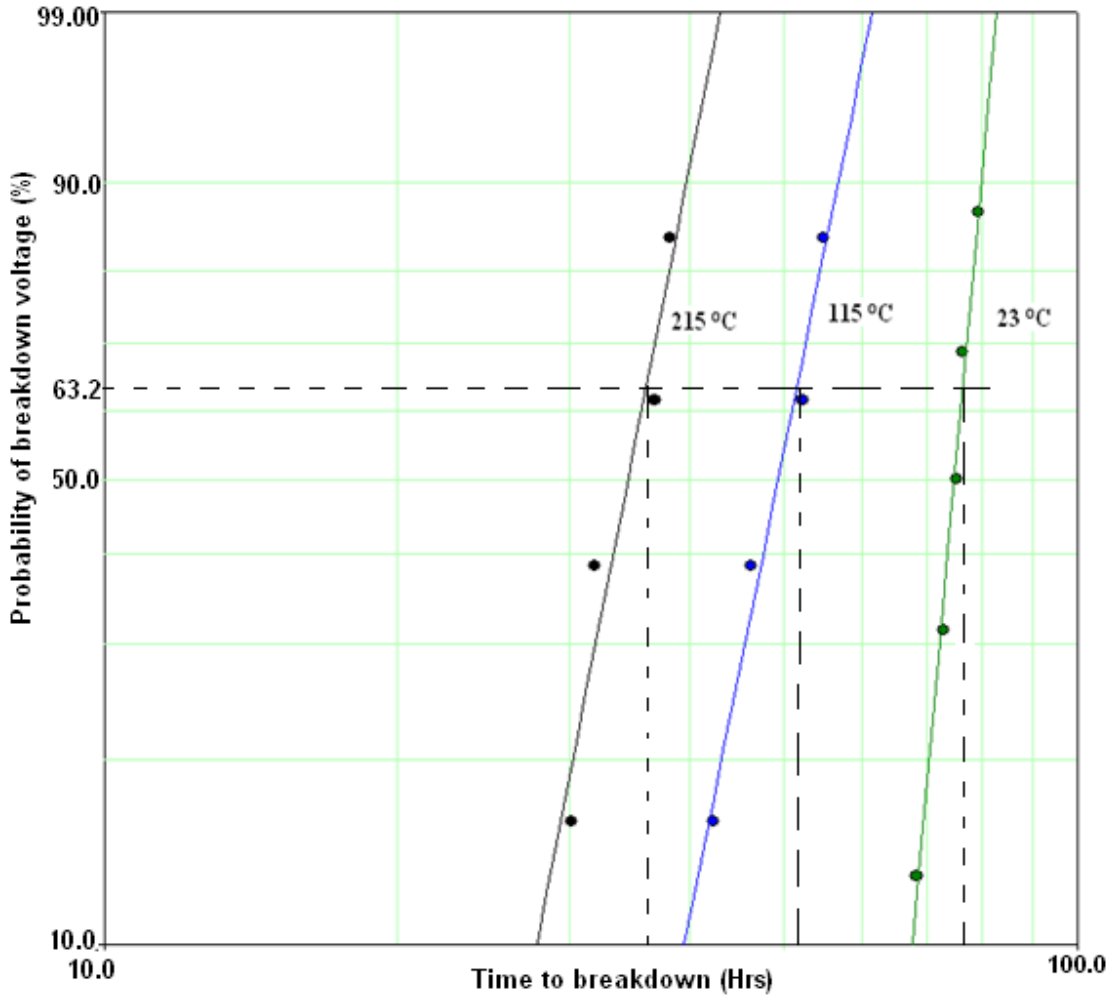

Figure 7.1 Weibull plots of 60 Hz breakdown voltage probability of twisted samples aged at 1.5 kV for temperatures of 23°C, 115°C, and 215°C

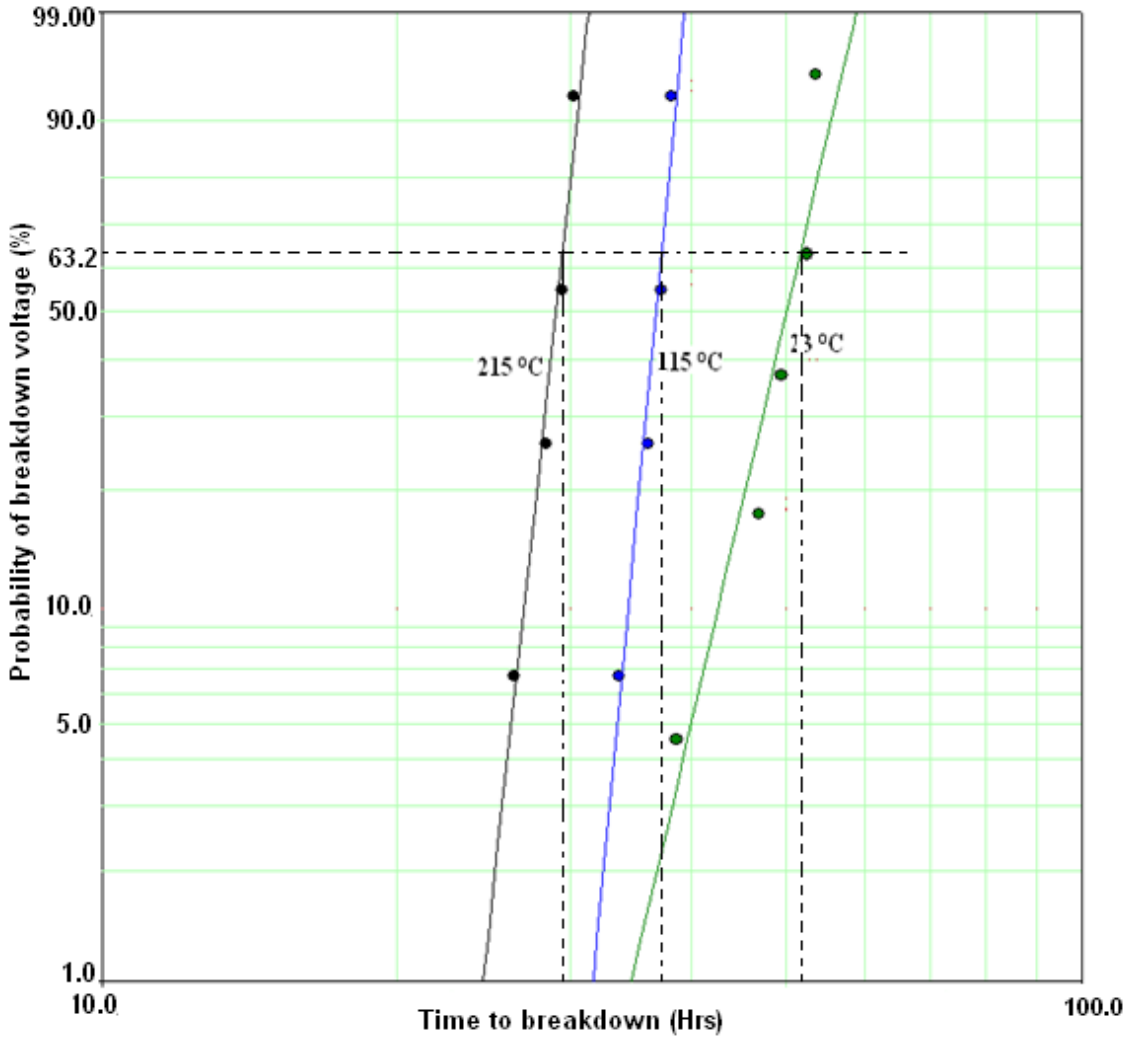

Figure 7.2 Weibull plots of 60 Hz breakdown voltage probability of twisted samples aged at 2 kV for temperatures of 23°C, 115°C, and 215°C

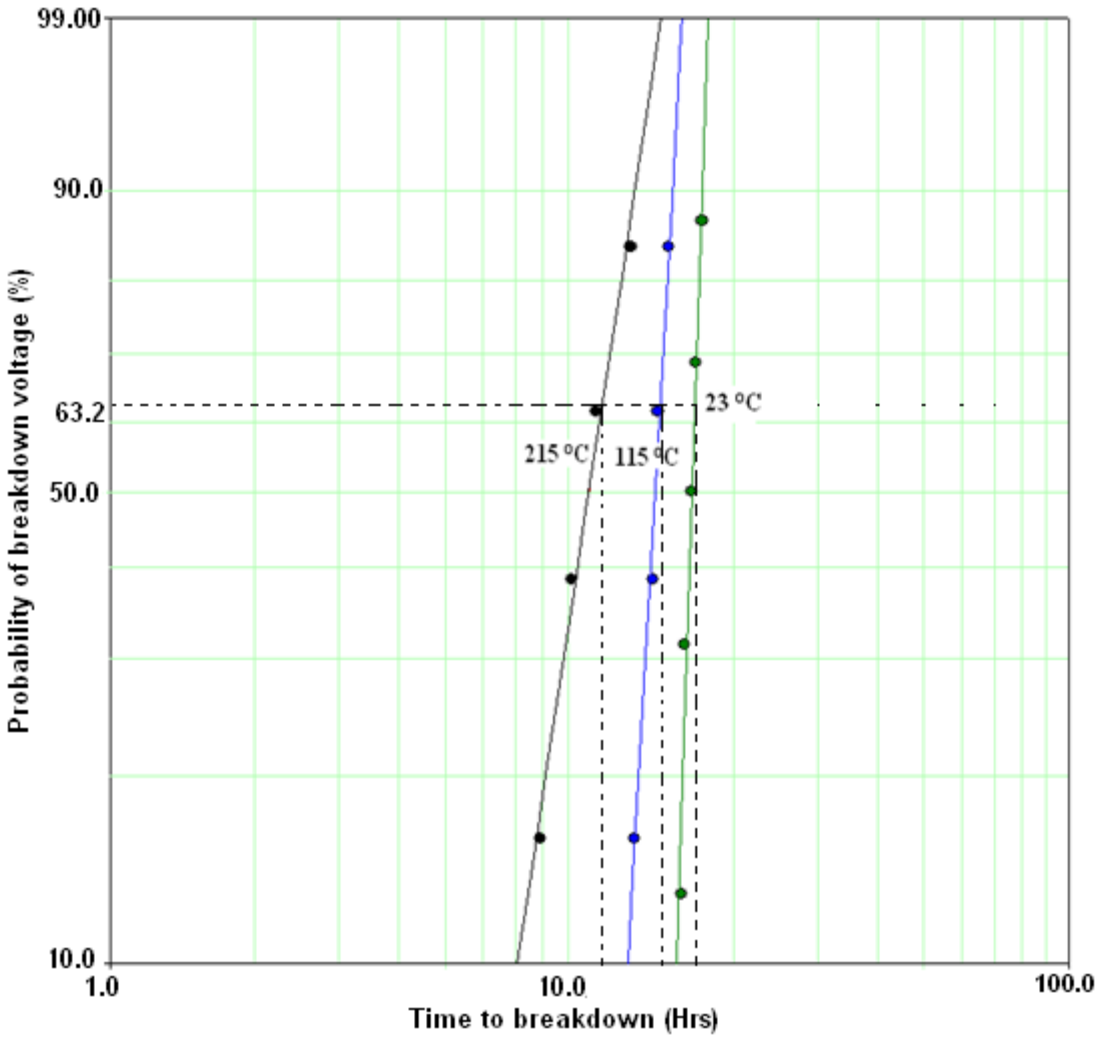

Figure 7.3 Weibull plots of 60 Hz breakdown voltage probability of twisted samples aged at 3 kV for temperatures of 23°C, 115°C, and 215°C

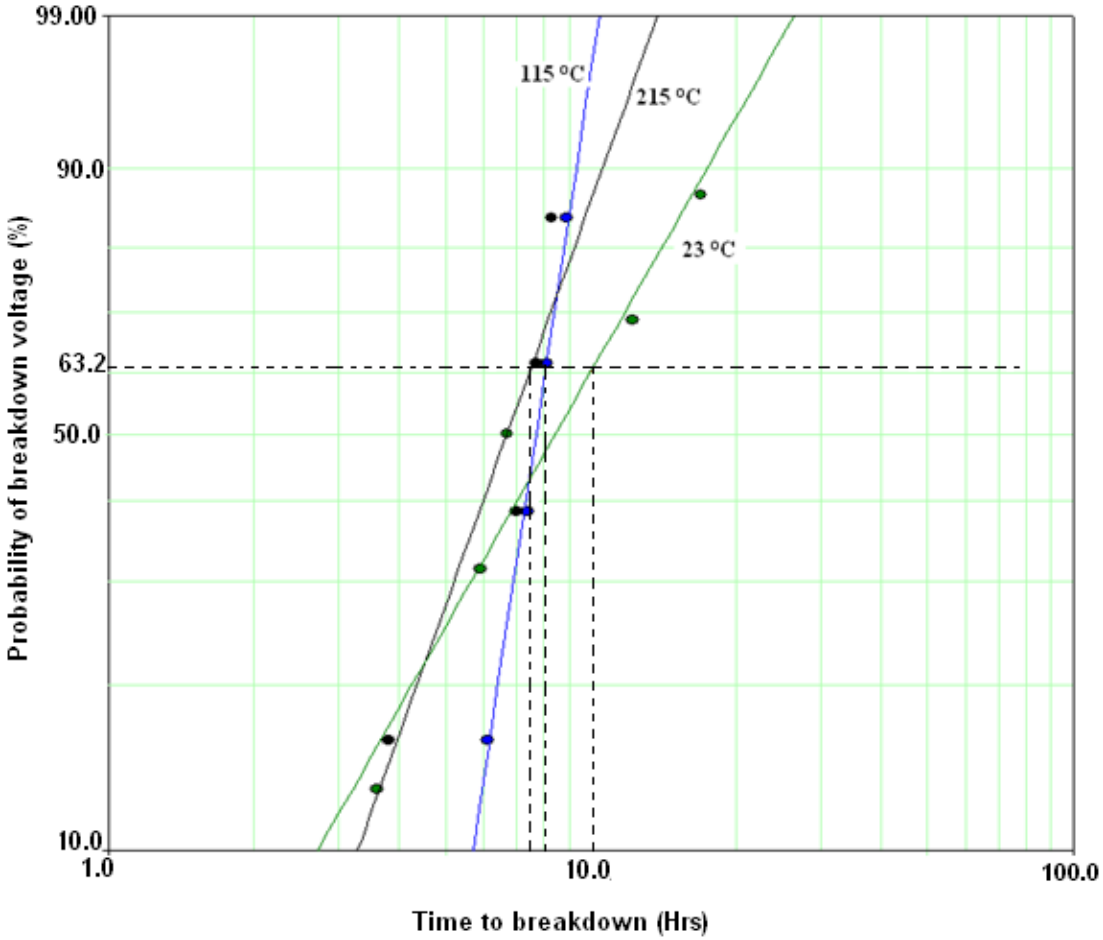

Figure 7.4 Weibull plots of 60 Hz breakdown voltage probability of twisted samples aged at 4 kV for temperatures of 23°C, 115°C, and 215°C

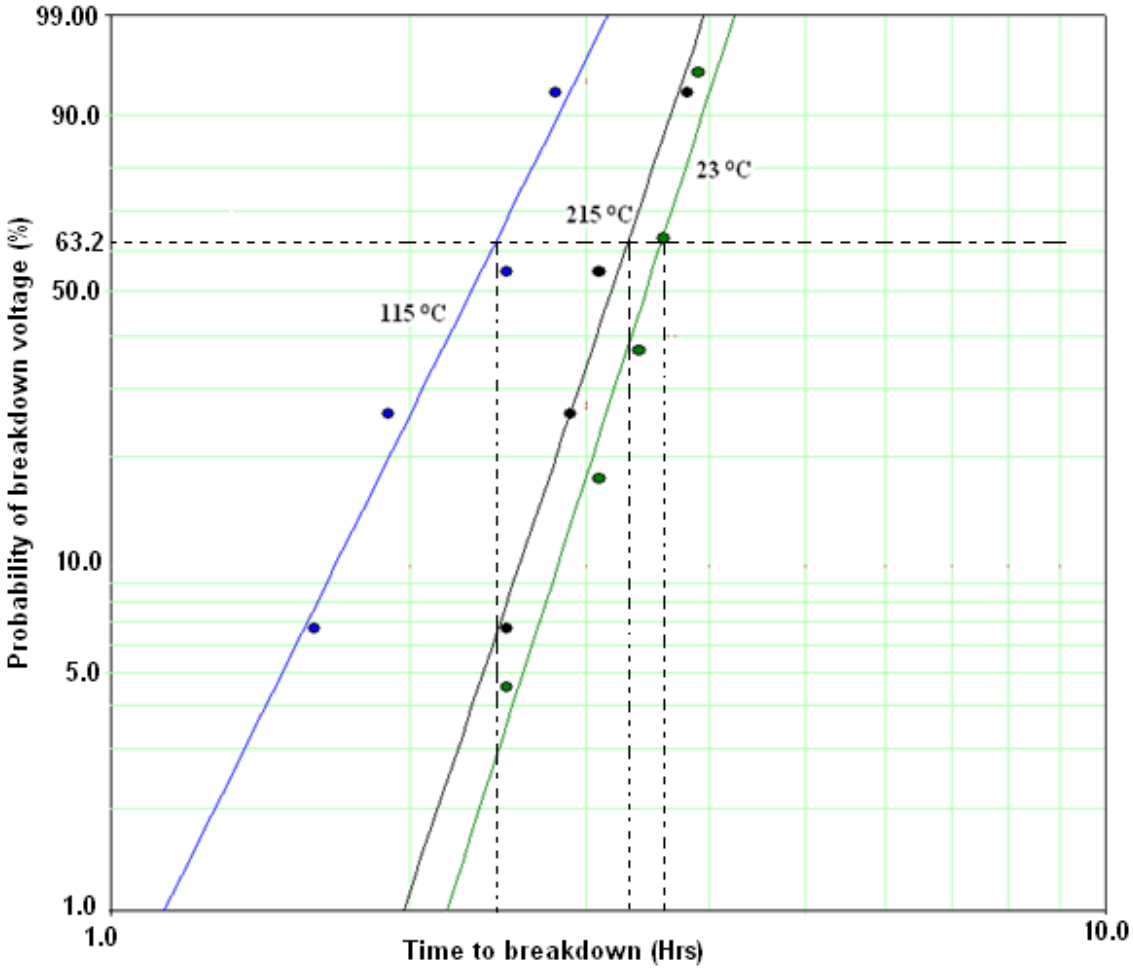

Figure 7.5 Weibull plots of 60 Hz breakdown voltage probability of twisted samples aged at 5 kV for temperatures of 23°C, 115°C, and 215°C

Table 7.1

Time to breakdown (63.2% probability) for MW 16-C insulation at different voltage levels

Applied Voltage (kV)	**Time to Breakdown (63.2% Probability)**		
	23°C	**115°C**	**215°C**
1.5	76.3	51.5	36.1
2.0	51.6	37.2	29.5
3.0	16.6	14.0	10.7
4.0	10.5	8.2	7.7
5.0	3.6	2.4	3.3

The time to breakdown for different probability of breakdown voltage are calculated from the given Weibull distribution plot at each voltage stress for different temperatures. Changes in the aging process with changes in voltage levels are also shown by the summarized *V*-t lifetime graphs presented in Figure 7.6. Here, the results fit very well to the inverse power law of Eq. 3.3, with the value of the exponent *n* increasing from 2.0 at room temperature to 2.7 at 215°C.

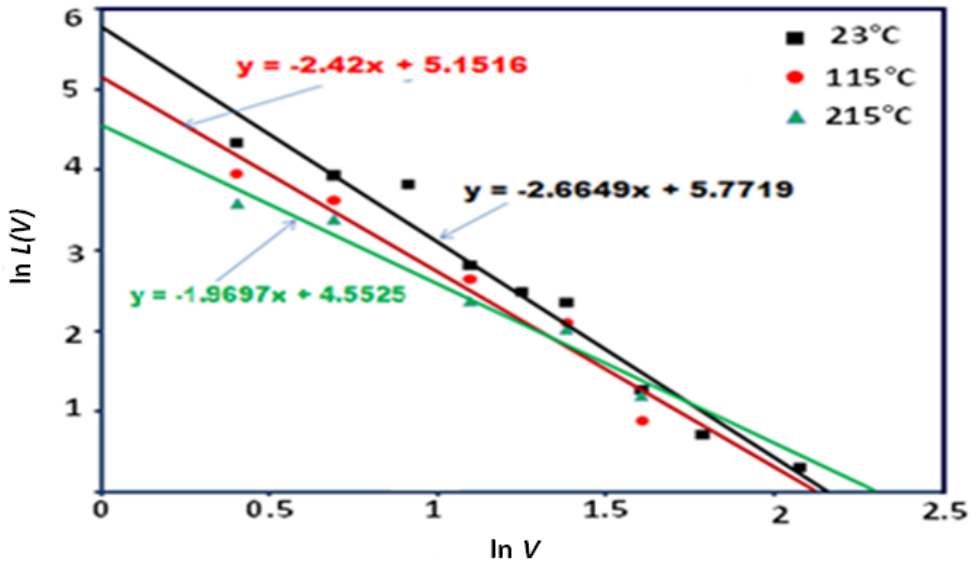

Figure 7.6 Measured time to breakdown time (hrs) at 63.2% probability of breakdown voltage at each voltage stress, plotted according to the inverse power law, Eq. (3-3) with y = ln *L(V)* and x = ln *V*

The graph is plotted between ln *L(V)* and ln *V*, where *L(V)* is time to breakdown at 63.2% probability of breakdown voltage obtained from the Weibull distribution and *V* is the applied voltage. From the graph, using the inverse power law, the lifetime model of MW 16-C insulation is obtained, which is presented in Table 7.2.

Table 7.2

Inverse power model of MW 16-C at different temperature

Aging Temperature	**Inverse Power Model**
23°C	$L(V) = 320 * V^{-2.66}$
115°C	$L(V) = 173 * V^{-2.42}$
215°C	$L(V) = 95 * V^{-1.97}$

Such change of the aging mechanism is also indicated by the Arrhenius plots of Figure 7.7. It is clearly demonstrated that the effect of increasing the test voltage from 1.5 kV to 5 kV is to reduce the apparent thermal activation energy from 4.7 to 0.7kJ/mol. In general, the temperature dependence of dielectric properties of polyimide films, as permittivity and dc conduction, is usually governed by activation energies in the range of 100 to150 kJ/mol [40]. This means that, in this case, thermally-activated processes of polyimide seem to have a minor effect on the rate of degradation.

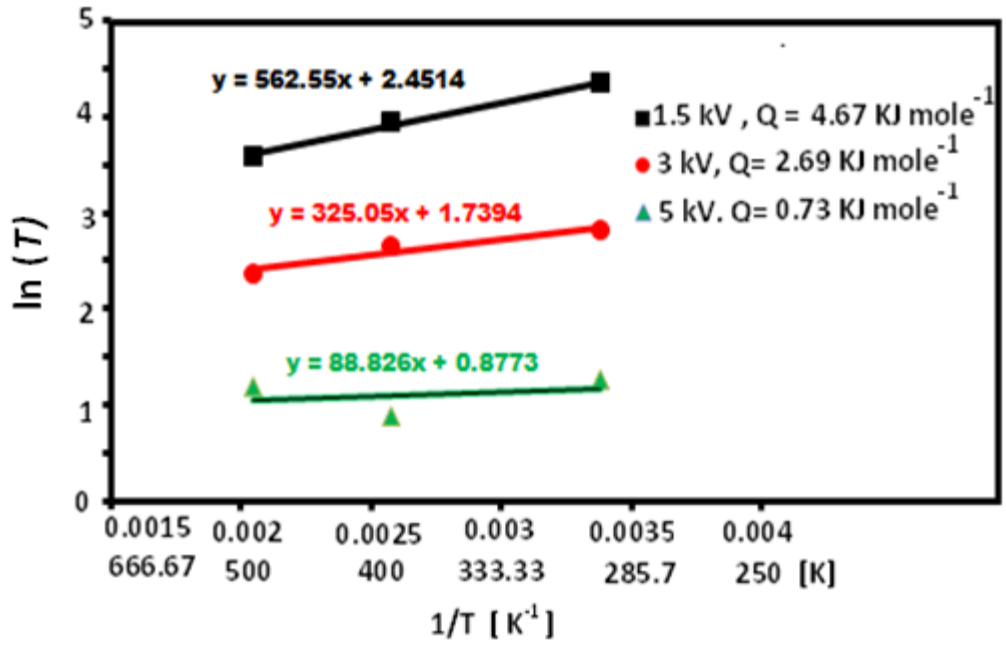

Figure 7.7 Effect of voltage stress on NEMA 16-C according to Arrhenius Eq. (3-7) with y = ln *L(T)* and x = 1/T

Results from measurements of the partial discharge characteristics are presented in Table 7.3 and Table 7.4. Figure 7.8 strongly indicates that this high aging rate of twisted pairs is likely caused by the large and increasing partial discharges occurring at

test voltages above approximately 3 kV. In comparison, the partial discharge level for single terminated wires with grounded electrode is found to be nearly constant after inception at about 0.5 kV.

Table 7.3

Average measured apparent partial discharge levels versus effective test voltage, for twisted pair of sample of NEMA 16-C

Sample	**Approx. applied voltage [kV]**	**Max. pd level ΔQ [pc]**	**Comment**
Twisted Pair sample	0.8	198	Inception voltage
	1.0	360	
	1.5	585	
	2.0	675	
	3.0	615	
	4.0	1125	
	5.0	1500	

Table 7.4

Average measured apparent partial discharge levels versus effective test voltage, for single terminated wire with sliver paint

Sample	**Approx. applied voltage [kV]**	**Max. pd level ΔQ [pc]**	**Comment**
Single terminated wire with silver paint	0.8	27	Inception voltage
	1.0	38	
	1.5	38	
	2	38	
	3	35	
	4	29	
	5	43	
	6	145	

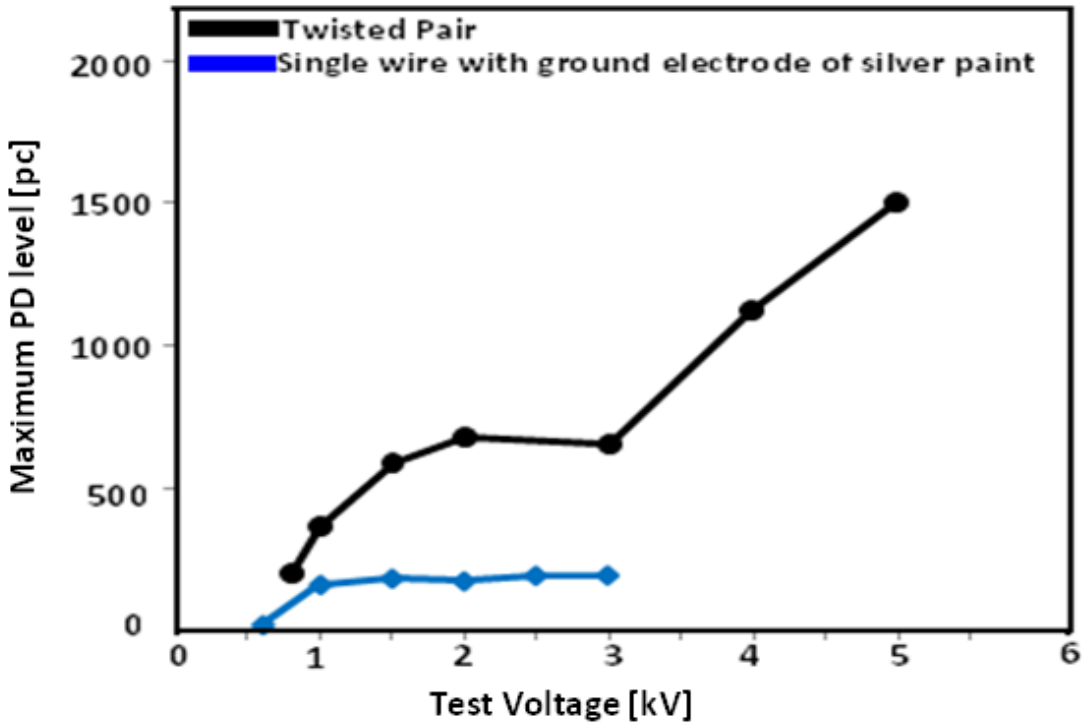

Figure 7.8 Average apparent partial discharge levels versus effective test voltage for the two test object

The partial discharge level is measured up to 5 kV for the twisted pair of samples, whereas measurements are only taken up to 3 kV for the single grounded and terminated samples. Based upon these observations, one should expect single wire samples with low partial discharge activity to have longer breakdown times than the twisted pairs at comparable voltage stress. This expectation is experimentally verified by the results presented in Figure 7.9. In case of single grounded and terminated wires, the time to breakdown at 2 kV is found to be 1.8 times larger than that of twisted pairs aged at the comparable voltage of 4 kV. The shape parameter β is also clearly higher, supporting the same expectation.

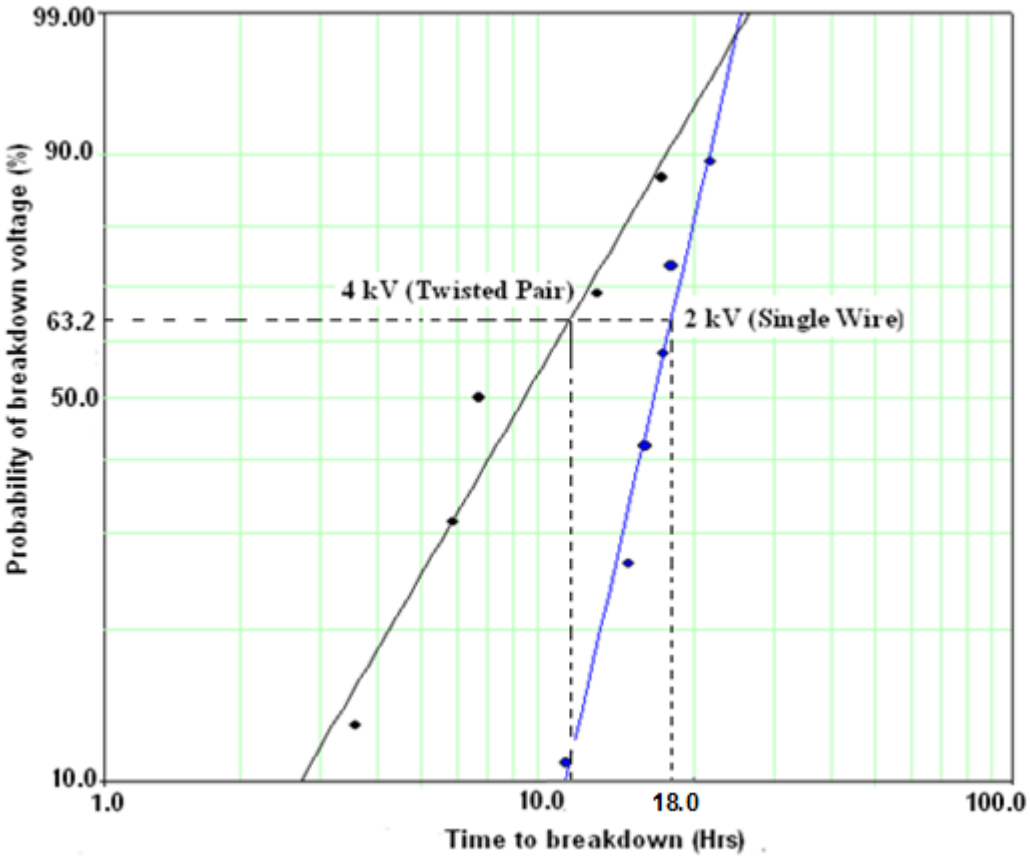

Figure 7.9 Weibull plot of 60 Hz breakdown probability of twisted pairs and single machine winding at room temperatures of 23°C and test voltages of 4 kV and 2 kV respectively

In a case like this where aging is characterized by change of the dominant mechanisms, extrapolation may easily lead to optimistic estimate of the expected lifetime at service conditions. A better estimate of lifetime of twisted wires would be certain to fit the results at each temperature to separate continuous straight lines for aging below and above 3 kV. When this is done, the graphs of Figure 7.6 became nearly parallel, with a value of n equal to 2.0 for test voltages below 3 kV and 2.9 at the highest test voltages at room temperature.

7.2 Aging with High Frequency Pulse Voltage

The time to breakdown measurements are performed with 60 Hz ac for polyimide insulated NEMA MW 16-C winding. The time to breakdown under high frequency pulse voltage is unable to obtain because the dielectric test system is not strong enough to withstand the fault condition. For the accelerated aging study with high frequency pulse voltage and temperature, evaluation of change in dielectric properties (partial discharge and breakdown voltage) is monitored versus the accelerated aging caused by the high frequency pulse voltage and temperature. The measurements of partial discharge and breakdown voltage are performed at power frequency of 60 Hz after accelerated aging.

Partial discharges and breakdown voltage are measured for five samples after 100, 200, 500, and 1000 hrs of accelerated aging. These measurements are also taken for new samples. Presented in these results are the following measurements:

7.2.1 Partial Discharge Measurements

- Partial discharge inception voltage (PDIV)
- Partial discharge extinction voltage (PDEV)
- Three dimensional (φ-q-n) analysis of partial discharge

7.2.1.1 Partial Discharge Inception Voltage (PDIV)

The average value and standard deviation for the five measured samples are calculated for the PDIV. Table 7.5 through Table 7.8 shows the result of maximum, average, and minimum PDIV record and standard deviation for four types of insulations

followed by the histograms which are subjected to accelerated aging with high frequency pulse voltages and high temperature.

The average and standard deviations of the five samples tested are calculated using the formulas;

Average:

$$\bar{x} = \frac{1}{N}\sum_{i=1}^{N} x_i \tag{7-2}$$

Standard Deviation:

$$\sigma = \sqrt{\left[\frac{1}{N}\sum_{i=1}^{N}(x_i - \bar{x})^2\right]} \tag{7-3}$$

where;

x = the values of partial discharge inception voltage

N = the number of sample tested

Table 7.5

Partial discharge inception voltage of MW 35-C accelerated aged by pulse voltage of 1300 V at 40 kHz and 180°C

Time of Accelerated Aging	Maximum PDIV (V)	Minimum PDIV (V)	Average PDIV (V)	Standard Deviation (σ)
Before Aging	800.0	730.0	774.0	24.5
100 hrs	840.0	720.0	786.0	38.8
500 hrs	790.0	770.0	780.0	10.0
1000 hrs	840.0	740.0	776.0	44.9

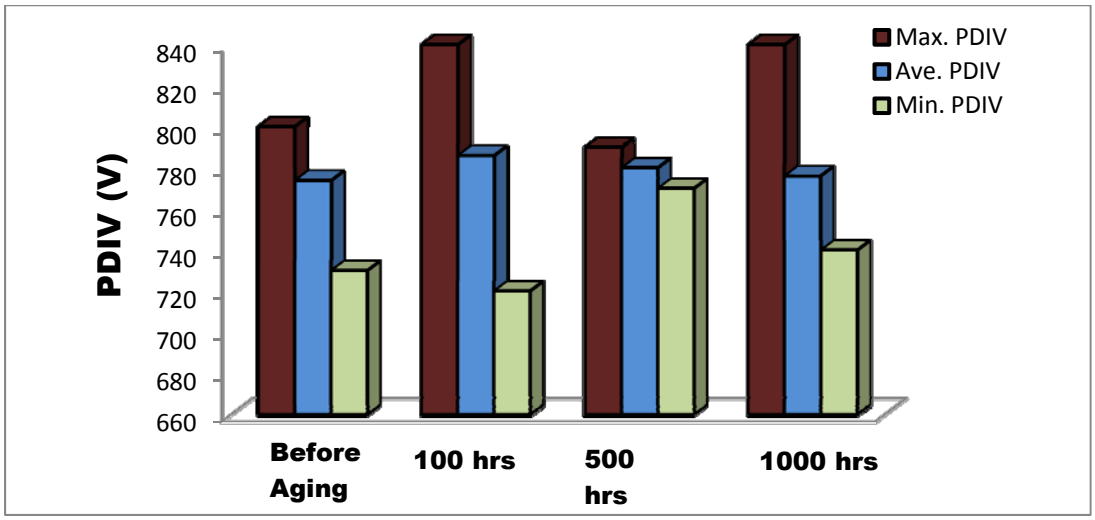

Figure 7.10 Partial discharge inception voltage of MW 35-C accelerated aged by pulse voltage of 1300 V at 40 kHz and 180°C

Table 7.6

Partial discharge inception voltage of MW 80-C accelerated aged by pulse voltage of 1300 V at 40 kHz and 140°C

Time of Accelerated Aging	Maximum PDIV (V)	Minimum PDIV (V)	Average PDIV (V)	Standard Deviation (σ)
Before Aging	720.0	690.0	702.0	11.6
100 hrs	770.0	690.0	728.0	24.3
500 hrs	750.0	690.0	717.0	23.8

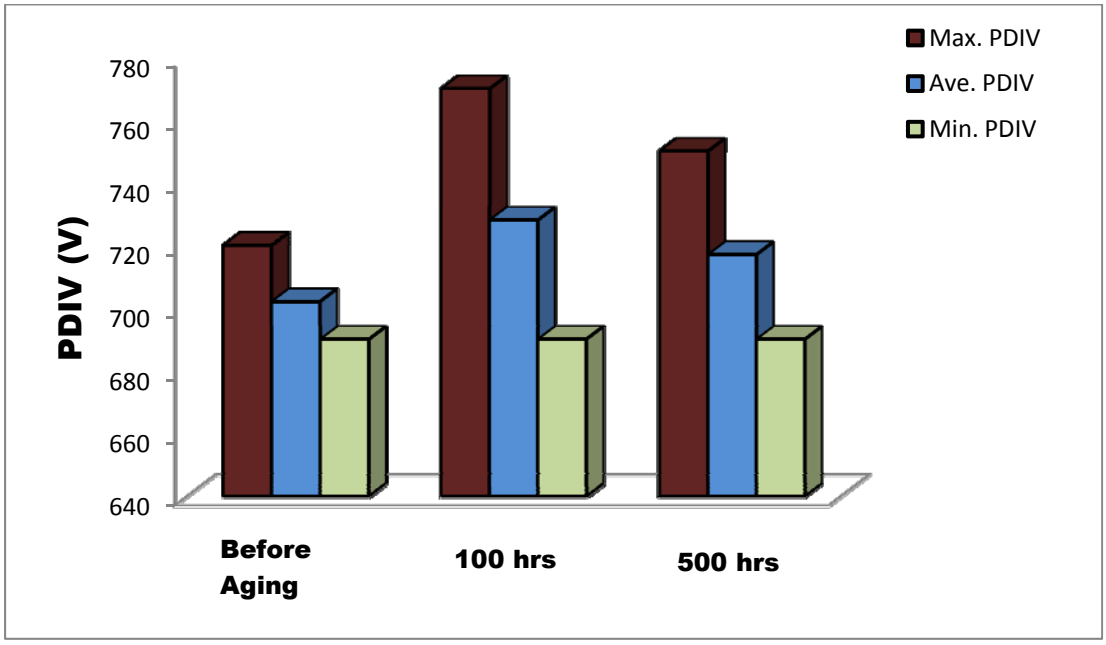

Figure 7.11 Partial discharge inception voltage of MW 80-C accelerated aged by pulse voltage of 1300 V at 40 kHz and 140°C

Table 7.7

Partial discharge inception voltage of MW 16-C accelerated aged by pulse voltage of 1350 V at 20 kHz and 216°C

Time of Accelerated Aging	Maximum PDIV (V)	Minimum PDIV (V)	Average PDIV (V)	Standard Deviation (σ)
Before Aging	750.0	720.0	734.0	10.2
100 hrs	780.0	740.0	750.0	15.6
200 hrs	770.0	730.0	746.0	13.3
500 hrs	680.0	590.0	652.0	32.7
1000 hrs	680.0	620.0	644.0	22.4

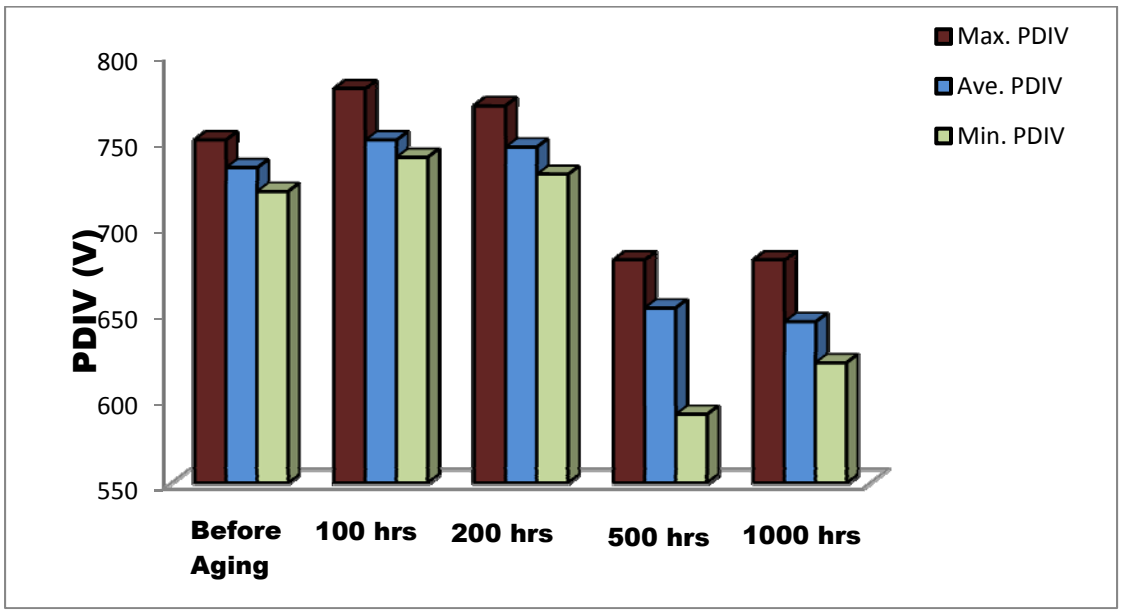

Figure 7.12 Partial discharge inception voltage of MW 16-C accelerated aged by pulse voltage of 1350 V at 20 kHz and 216°C

Table 7.8

Partial discharge inception voltage of MW 73-C accelerated aged by pulse voltage of 1350 V at 20 kHz and 200°C

Time of Accelerated Aging	Maximum PDIV (V)	Minimum PDIV (V)	Average PDIV (V)	Standard Deviation (σ)
Before Aging	670.0	620.0	644.0	16.3
100 hrs	680.0	620.0	653.0	19.4
200 hrs	660.0	590.0	640.0	26.0
500 hrs	640.0	610.0	624.0	10.2
1000 hrs	630.0	590.0	610.0	14.14

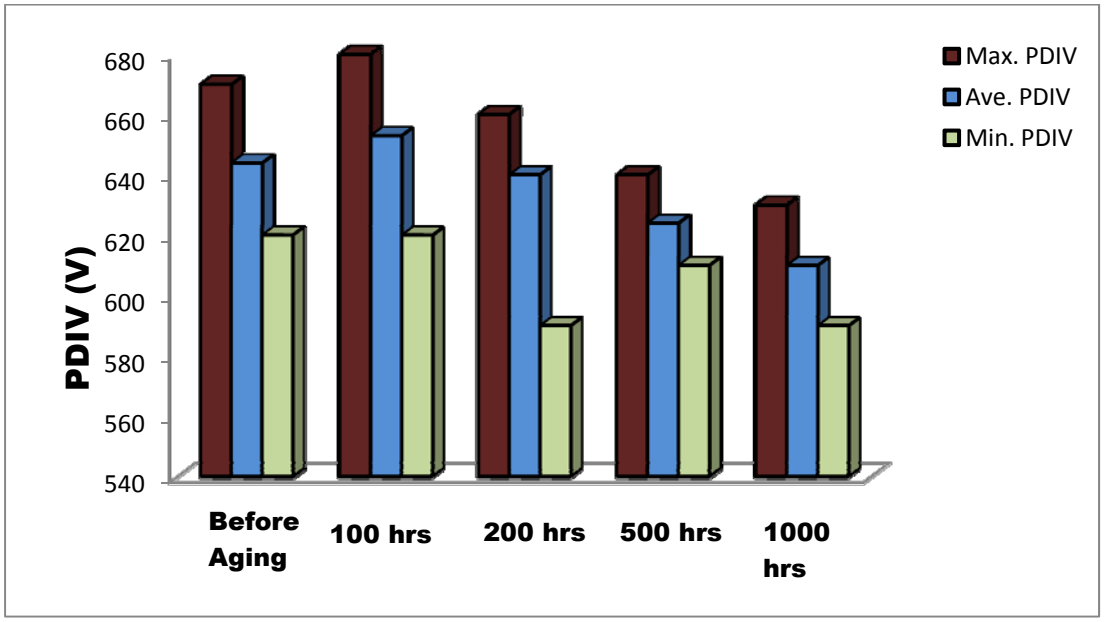

Figure 7.13 Partial discharge inception voltage of MW 73-C accelerated aged by pulse voltage of 1350 V at 20 kHz and 200°C

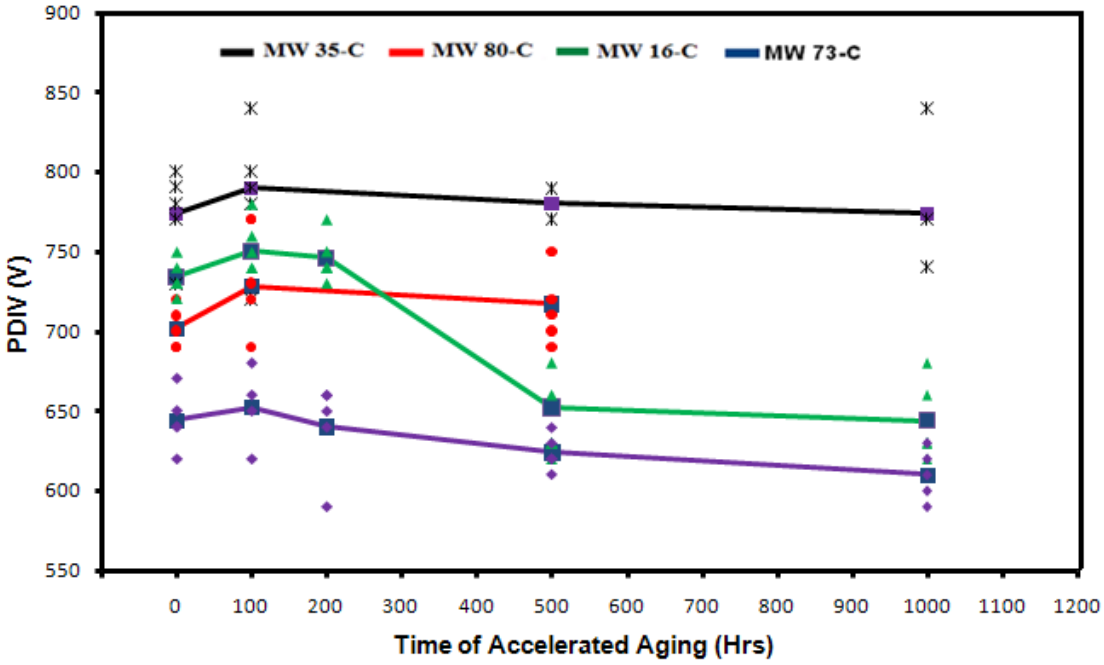

Figure 7.14 Partial discharge inception voltage (PDIV) at 60 Hz ac as function of time of accelerated aging

Partial discharge inception voltage (PDIV) is shown in Figure 7.14. Partial discharge inception voltage shows a similar variation for the MW 80-C, MW 35-C, MW 16-C, and MW 73-C wire insulation. PDIV increases at 100 hrs of accelerated aging and reduces with longer duration of accelerated aging. The increased value of PDIV is related to the initial conditioning of the insulation material under multiple stresses.

The results for partial discharge show decreasing of the inception voltage with the longer accelerated aging of 500 hrs and 1000 hrs. The insulation of the samples MW 80-C break at approximately 700 hrs of the accelerated aging, and therefore, Figure 5.5 does not present the results for 1000 hrs of aging. For MW 16-C insulation, partial discharge inception voltages change significantly from 200 hrs to 500 hrs of accelerated

degradation, and later show d resistance to high frequency pulse voltage and high temperature until 1000 hrs.

The ratio between the dielectric constants of the insulation and the gas determines the electric field strength in the microvoids that exist in the insulation [20]. After the sample is aged for 100 hrs, the partial discharge activity increases the conductivity on the surface of microvoids and the insulation surface. For long-aged samples when the surface conductivity becomes higher, some defects or byproducts are formed in the microvoids imperfection due to partial discharge phenomena. The charge migration in the microvoids surface leads to an increase in the inception voltage [41 and 42], which is verified by the increase in inception voltage for all four types of insulating materials after 100 hrs of accelerated aging.

7.2.1.2 Partial Discharge Extinction voltage (PDEV)

The average value and standard deviation for the five measured samples are calculated for partial discharge extinction voltage. Table 7.9 through Table 7.12 shows the result of the maximum PDEV, average PDEV, and minimum PDEV recorded and standard deviation for all four types of insulations which are subjected to accelerated aging with high frequency pulse voltages and high temperature. The tables are followed by the histograms.

The average value and standard deviations of the five tested samples are calculated using the same formula used for partial discharge inception voltage.

Table 7.9

Partial discharge extinction voltage of MW 35-C accelerated aged by pulse voltage of 1300 V at 40 kHz and 180°C

Time of Accelerated Aging	Max. PDEV (V)	Min. PDEV (V)	Average PDEV (V)	Standard Deviation (σ)
Before Aging	760.0	690.0	744.0	15.2
100 hrs	760.0	700.0	734.0	26.1
500 hrs	740.0	700.0	724.0	15.2
1000 hrs	710.0	690.0	706.0	6.5

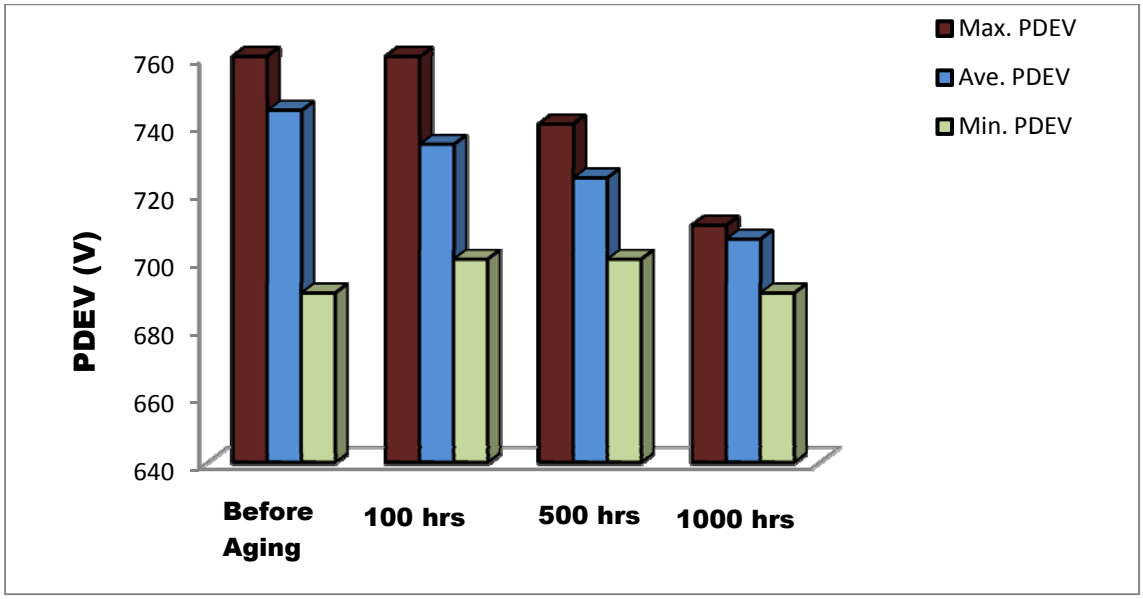

Figure 7.15 Partial discharge extinction voltage of MW 35-C accelerated aged by pulse voltage of 1300 V at 40 kHz and 180°C

Table 7.10

Partial discharge extinction voltage of MW 80-C accelerated aged by pulse voltage of 1300 V at 40 kHz and 140°C

Time of Accelerated Aging	Max. PDEV (V)	Min. PDEV (V)	Average PDEV (V)	Standard Deviation (σ)
Before Aging	670.0	640.0	656.0	11.4
100 hrs	700.0	630.0	665.0	29.7
500 hrs	650.0	610.0	632.0	20.5

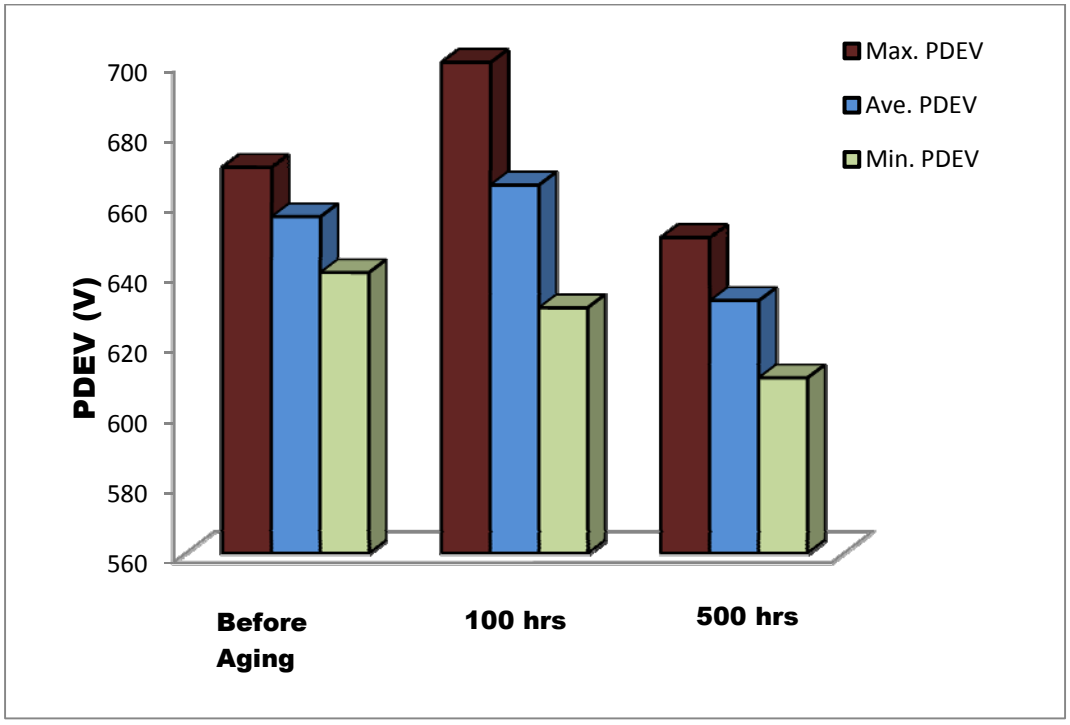

Figure 7.16 Partial discharge extinction voltage of MW 80-C accelerated aged by pulse voltage of 1300 V at 40 kHz and 140°C

Table 7.11

Partial discharge extinction voltage of MW 16-C accelerated aged by pulse voltage of 1350 V at 20 kHz and 216°C

Time of Accelerated Aging	Max. PDEV (V)	Min. PDEV (V)	Average PDEV (V)	Standard Deviation (σ)
Before Aging	690.0	660.0	678.0	10.3
100 hrs	720.0	670.0	690.0	10.2
200 hrs	720.0	670.0	692.0	17.5
500 hrs	640.0	540.0	600.0	33.8
1000 hrs	620.0	590.0	604.0	10.2

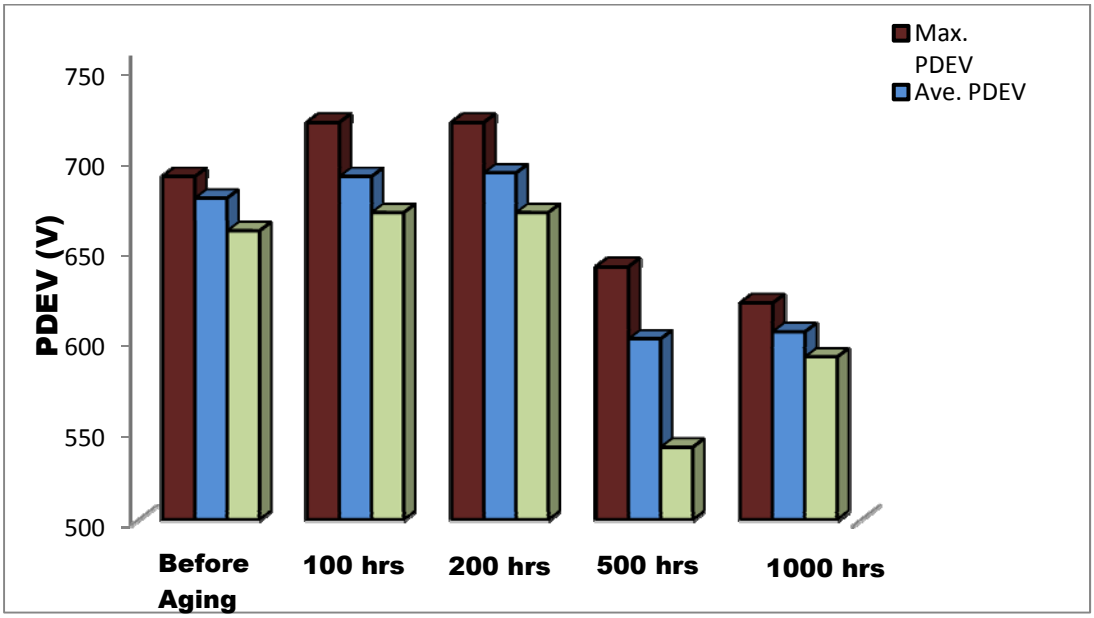

Figure 7.17 Partial discharge extinction voltage of MW 16-C accelerated aged by pulse voltage of 1350 V at 20 kHz and 216°C

Table 7.12

Partial discharge extinction voltage of MW 73-C accelerated aged by pulse voltage of 1350 V at 20 kHz and 200°C

Time of Accelerated Aging	Max. PDEV (V)	Min. PDEV (V)	Average PDEV (V)	Standard Deviation (σ)
Before Aging	610.0	590.0	602.0	7.5
100 hrs	600.0	570.0	587.0	13.0
200 hrs	620.0	550.0	596.0	25.8
500 hrs	600.0	560.0	582.0	13.3
1000 hrs	600.0	550.0	576.0	18.54

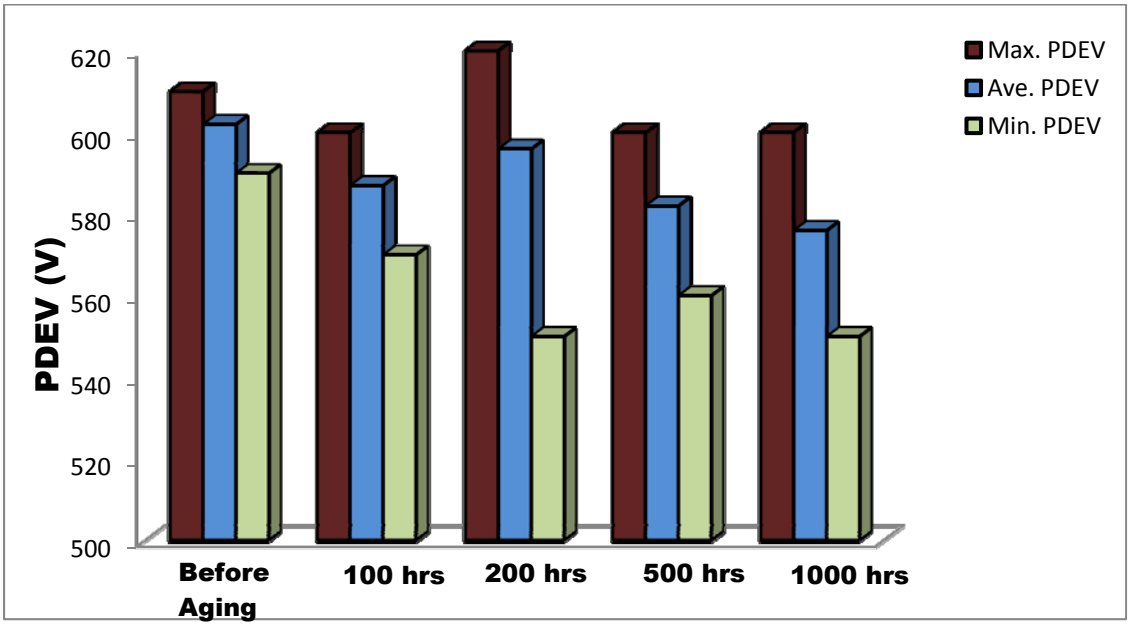

Figure 7.18 Partial discharge extinction voltage of MW 73-C accelerated aged by pulse voltage of 1350 V at 20 kHz and 200°C

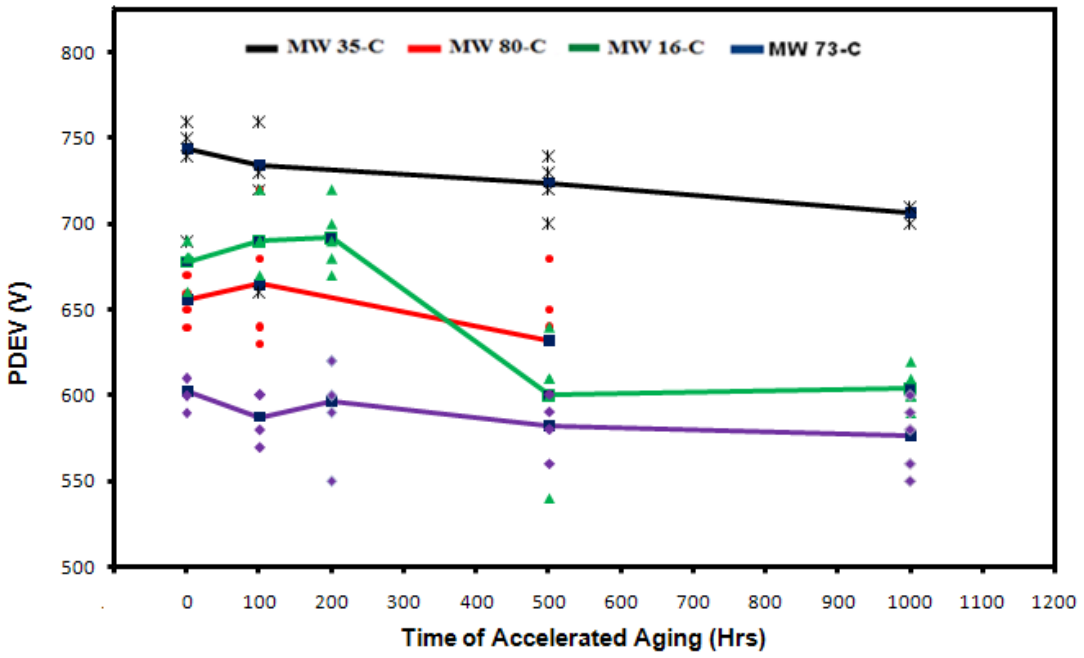

Figure 7.19 Partial discharge extinction voltage (PDEV) at 60 Hz ac as function of time of accelerated aging

Partial Discharge extinction voltage is shown in Figure 5.10. The partial discharge extinction voltage is reduced gradually with accelerated aging for MW 35-C insulation. A similar trend is also seen with MW 73-C insulation. For MW 73-C, PDEV decreases after 100 hrs of accelerated aging with a slight increase in value after 200 hrs. For MW 80-C and MW 16-C insulation, the partial discharge extinction voltages show an identical trend to partial discharge inception voltage; i.e. it increases after 100 hrs of accelerated degradation and decreases with longer degradation. In all the cases, as the accelerated aging period exceeded 100 hrs, the measured partial discharge inception and partial discharge extinction voltages are lowered.

Partial discharge (inception/extinction) values of the MW 35-C were consistently greater than those of MW 80-C, MW 16-C, and MW 73-C. The high value of partial

discharge inception/extinction voltage for MW 35-C is due to the polyamideimide coating on a polyester layer which resist partial discharge on the surface of the insulation. The insulation of the MW 35-C shows the better electrical performance in terms of partial discharge inception and extinction voltages.

7.2.1.3 Three-Dimensional (φ-q-n) Analysis

Measurement of the partial discharge is performed using DDX 7000 detector and visualized in a 3-D pattern to observe the aging phenomena comprehensively. Figure 7.20 through Figure 7.23 present the φ-q-n (φ: phase, q: partial discharge magnitude, n: partial discharge pulse count) pattern of MW 35-C for the partial discharge measured at 750 V, 60 Hz ac. Partial discharge measurements are recorded for a total 6 second, 360 cycle. Figure 7.20 shows the highest partial discharge count at a lower magnitude of charge (q). This is the new sample without aged condition, so some defects and microvoids remain during the manufacturing process resulting in a high value of partial discharge count with lower magnitude of charge. Figure 7.21 shows the partial discharge parameters after aging for 100 hrs with high charge magnitude (q) for small pulse count of partial discharge. This result corresponds to the measurement of the partial discharge which shows an increasing inception voltage after 100 hrs of accelerated aging. The reduced number of pulse counts with an increase in charge magnitude corresponds to increase value of partial discharge inception voltage. Figure 7.22 and figure 7.23 show a partial discharge patterns similar to figure 7.20, but with lower pulse counts than shown in figure 7.20.

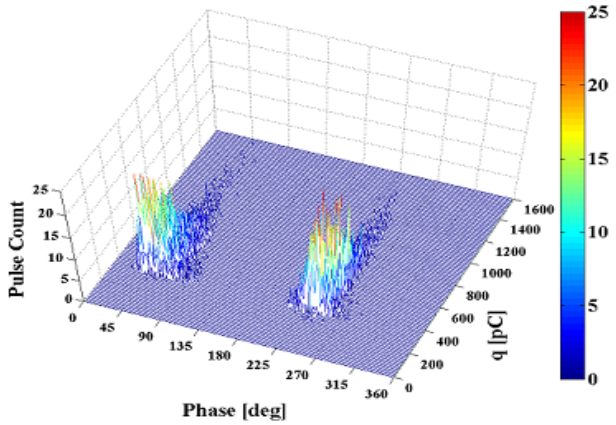

Figure 7.20 φ-q-n pattern of MW 35-C insulation at 750 V, 60 Hz ac, new sample, no aged

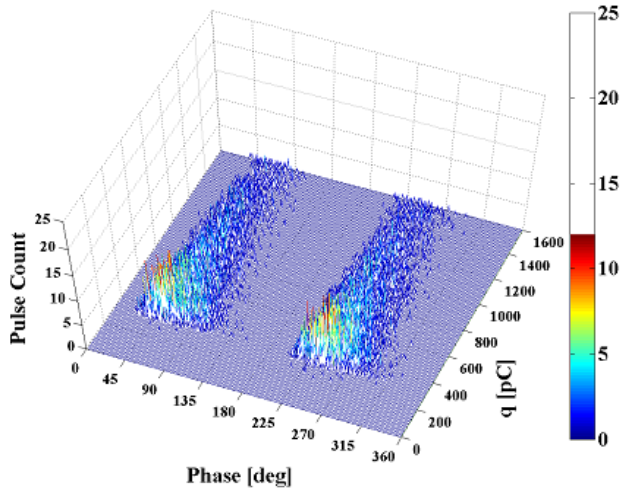

Figure 7.21 φ-q-n pattern of MW 35-C insulation at 750 V, 60 Hz ac, aged at: 100 hrs, 1300 V, 40 kHz and 180°C

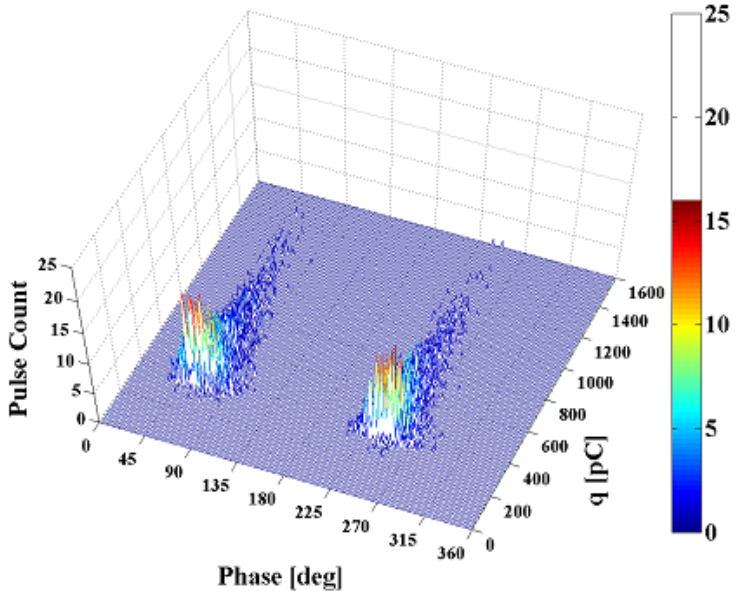

Figure 7.22 φ-q-n pattern of MW 35-C insulation at 750 V, 60 Hz ac, aged at: 500 hrs, 1300 V, 40 kHz and 180°C

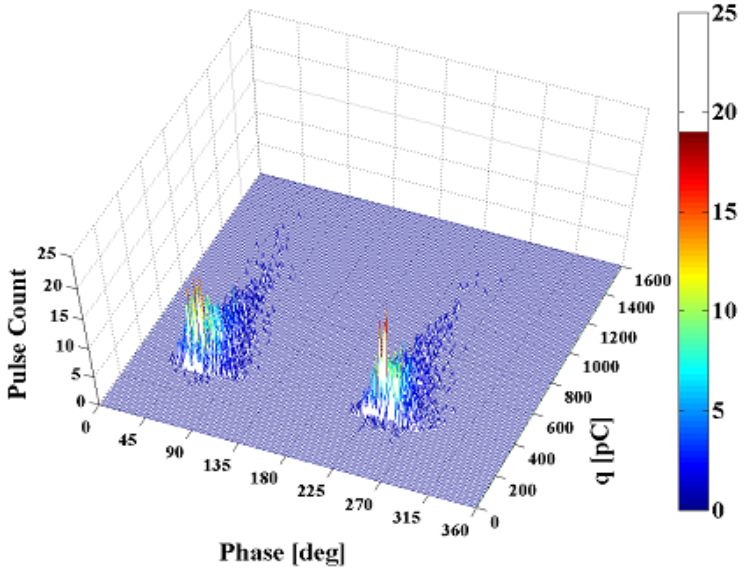

Figure 7.23: φ-q-n pattern of MW 35-C insulation at 750 V, 60 Hz ac, aged at: 1000 hrs, 1300 V, 40 kHz and 180ºC

7.2 AC Breakdown Measurement Results

The breakdown voltage measurements are taken for the twisted pair of samples after the partial discharge measurement. Table 7.13 through Table 7.16 shows the result of the maximum, average, and minimum breakdown voltage recorded and standard deviation for all four types of insulations subject to accelerated aging with high frequency pulse voltages and high temperature. The tables are followed by the histograms.

The average and standard deviations of five samples tested are calculated using the same formula used for partial discharge inception and partial discharge extinction voltage.

Table 7.13

Breakdown voltage of MW 35-C accelerated aged by pulse voltage of 1300 V at 40 kHz and 180°C

Time of Accelerated Aging	Max. Breakdown Voltage (kV)	Min. Breakdown Voltage (kV)	Average Breakdown Voltage(kV)	Standard Deviation (σ)
Before Aging	13.55	11.79	12.75	0.7
100 hrs	15.66	13.72	14.6	0.65
500 hrs	12.93	9.63	11.27	1.18
1000 hrs	10.34	6.65	8.47	1.5

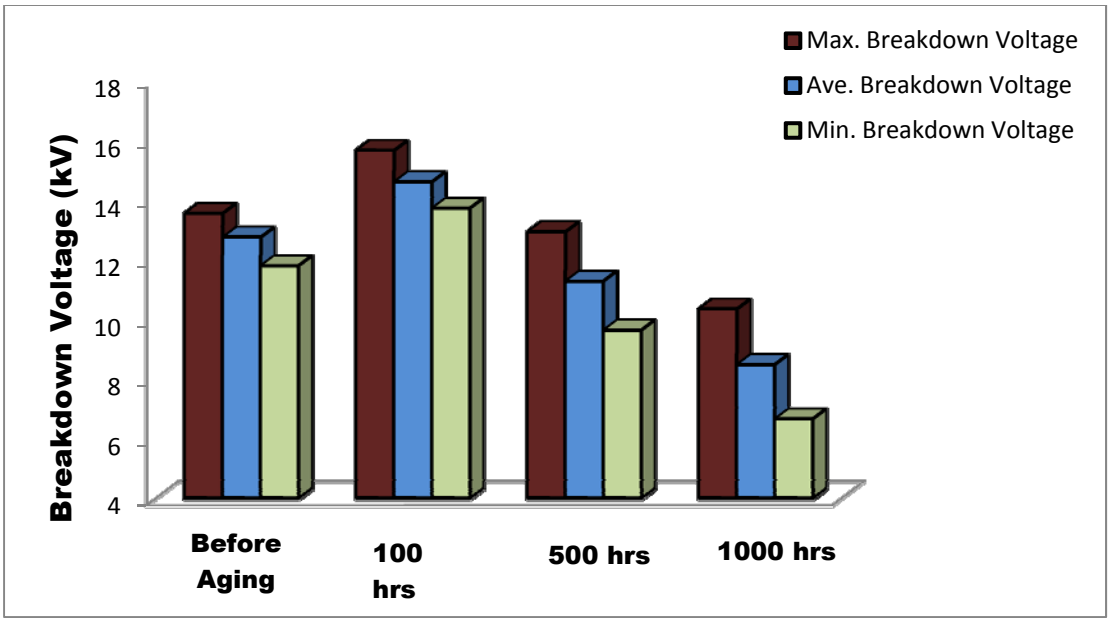

Figure 7.24…Breakdown voltage of MW 35-C accelerated aged by pulse voltage of 1300 V at 40 kHz and 180°C

Table 7.14

Breakdown voltage of MW 80-C accelerated aged by pulse voltage of 1300 V at 40 kHz and 140°C

Time of Accelerated Aging	Max. Breakdown Voltage (kV)	Min. Breakdown Voltage (kV)	Average Breakdown Voltage(kV)	Standard Deviation (σ)
Before Aging	13.29	11.43	11.92	0.72
100 hrs	13.5	10.62	12.00	1.04
500 hrs	12.6	10.6	11.8	0.71

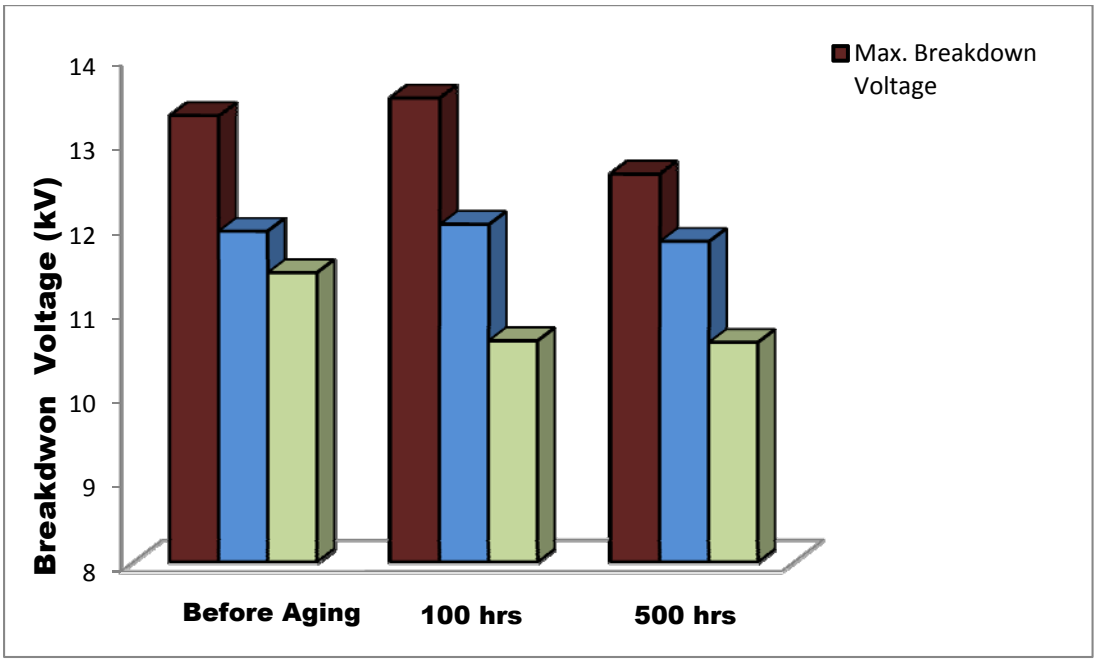

Figure 7.25 Breakdown voltage of MW 80-C accelerated aged by pulse voltage of 1300 V at 40 kHz and 140 °C

Table 7.15

Breakdown voltage of MW 16-C accelerated aged by pulse voltage of 1350 V at 20 kHz and 216°C

Time of Accelerated Aging	Max. Breakdown Voltage (kV)	Min. Breakdown Voltage (kV)	Average Breakdown Voltage(kV)	Standard Deviation (σ)
Before Aging	18.02	16.1	16.96	0.72
100 hrs	18.6	15.61	17.50	1.03
200 hrs	17.65	16.84	17.22	0.3
500 hrs	16.4	12.59	15.40	1.42
1000 hrs	16.6	14.2	14.86	1.03

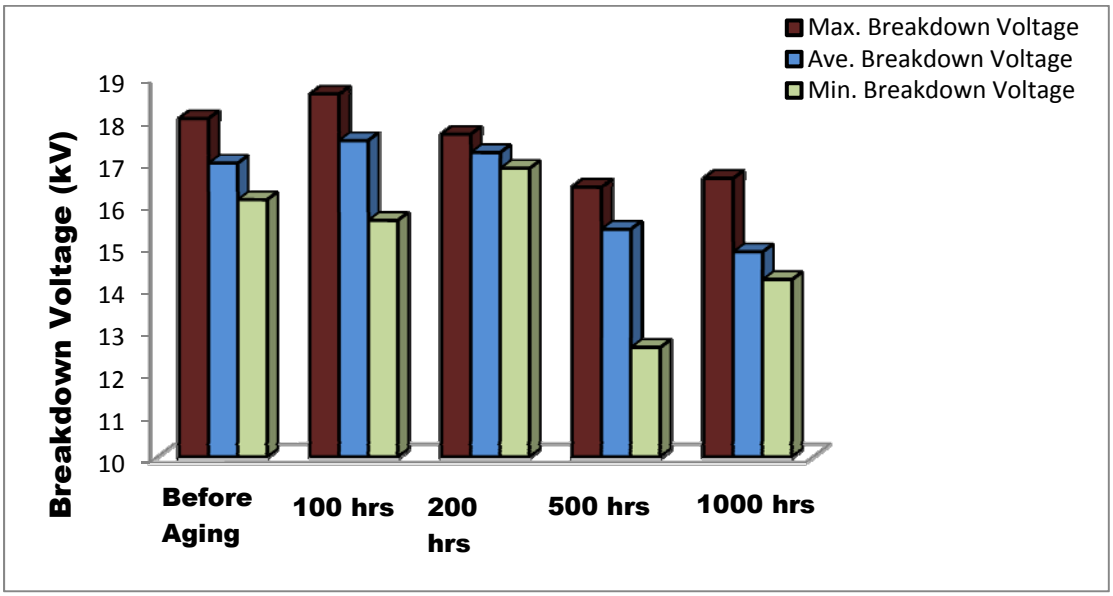

Figure 7.26 Breakdown voltage of MW 16-C accelerated aged by pulse voltage of 1350 V at 20 kHz and 216°C

Table 7.16

Breakdown voltage of MW 73-C accelerated aged by pulse voltage of 1350 V at 20 kHz and 200°C

Time of Accelerated Aging	Max. Breakdown Voltage (kV)	Min. Breakdown Voltage (kV)	Average Breakdown Voltage(kV)	Standard Deviation (σ)
Before Aging	16.71	13.38	15.27	1.23
100 hrs	15.43	10.16	12.43	2.32
200 hrs	16.2	12.20	13.92	1.49
500 hrs	14.6	10.29	11.88	1.48
1000 hrs	12.7	9.4	11.76	1.21

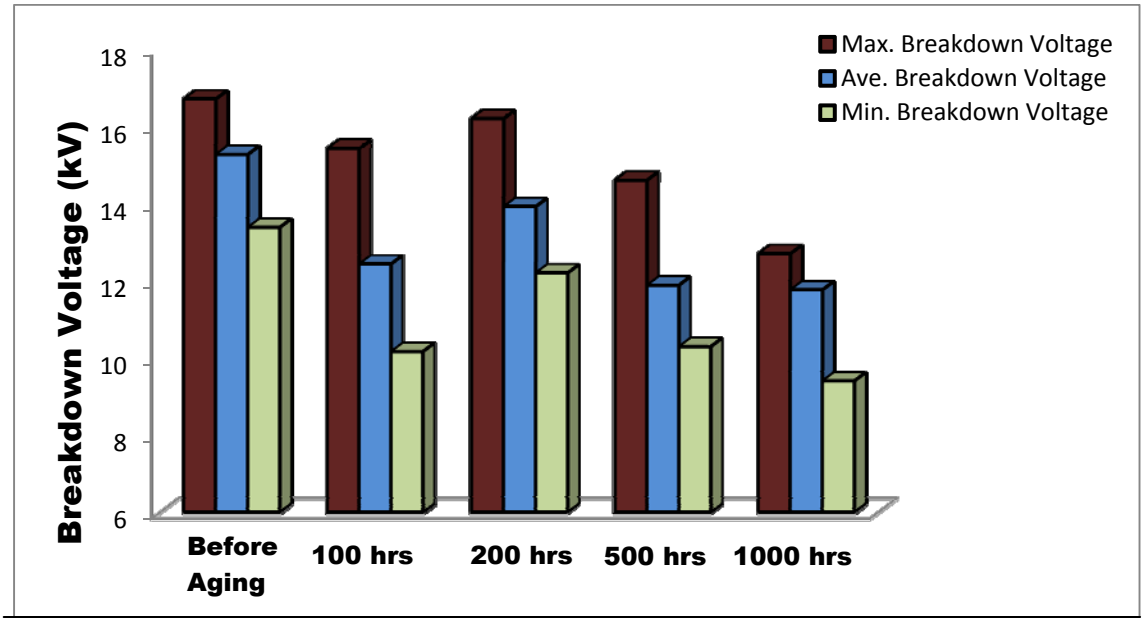

Figure 7.27 Breakdown voltage of MW 73-C accelerated aged by pulse voltage of 1350 V at 20 kHz and 200°C

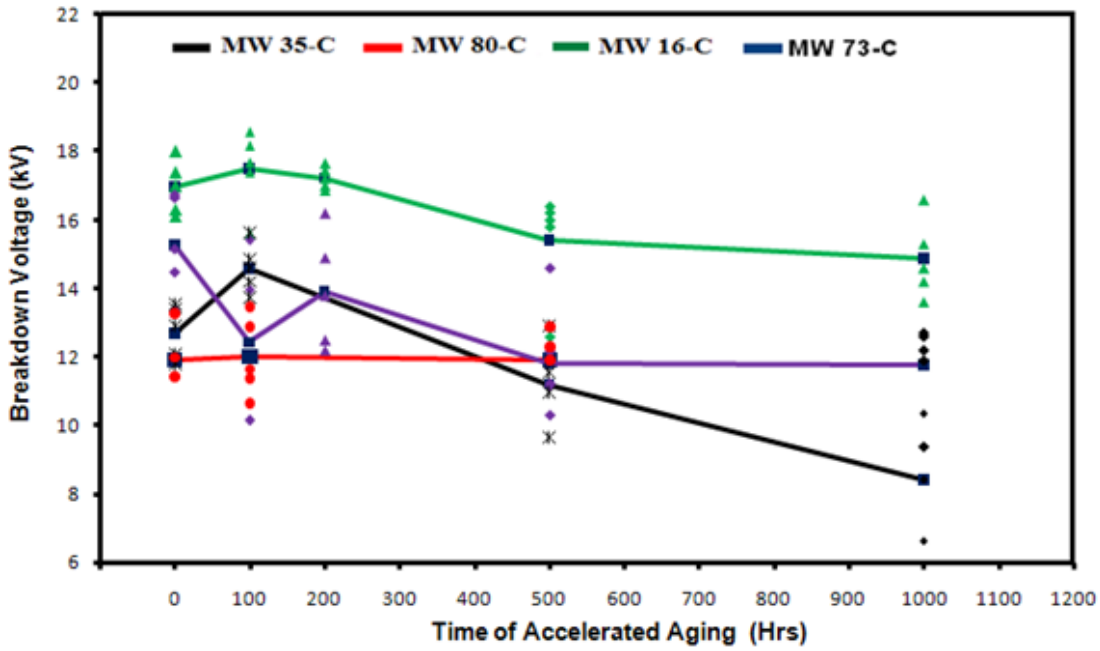

Figure 7.28 Breakdown voltage at 60 Hz ac as a function of time of accelerated aging

Breakdown voltage of MW 35-C and MW 16-C insulation show the similar trends. For MW 35-C and MW 16-C insulation, the breakdown voltage increases for accelerated aging duration of 100 hrs. Then, the breakdown voltage drops linearly for the samples accelerated aged for 500 hrs and 1000 hrs. The breakdown voltages for MW 80-C and MW 73-C have different trend. The breakdown voltage of MW 80-C does not change with an increase in time of aging. For MW 73-C, breakdown voltage decreases after 100 hrs of aging with an increment in 200 hrs. The breakdown voltage of MW 73-C at 200 hrs is still lower than that of the new sample. When compared with four types of insulation, the breakdown voltage measurement varies with time of accelerated aging. The MW 16-C shows the highest breakdown strength when compared with other insulations, although its partial discharge activity is lower than that of MW 35-C. This is

due to the polyimide insulation which is thermal resistant and shows high quality thermal behavior at an elevated temperature of 216°C.

The variation in breakdown voltage can be visualized with the help of Figure 7.29. The figure shows the cross section area of a twisted pair of samples and the corresponding surface of the insulation before and after aging.

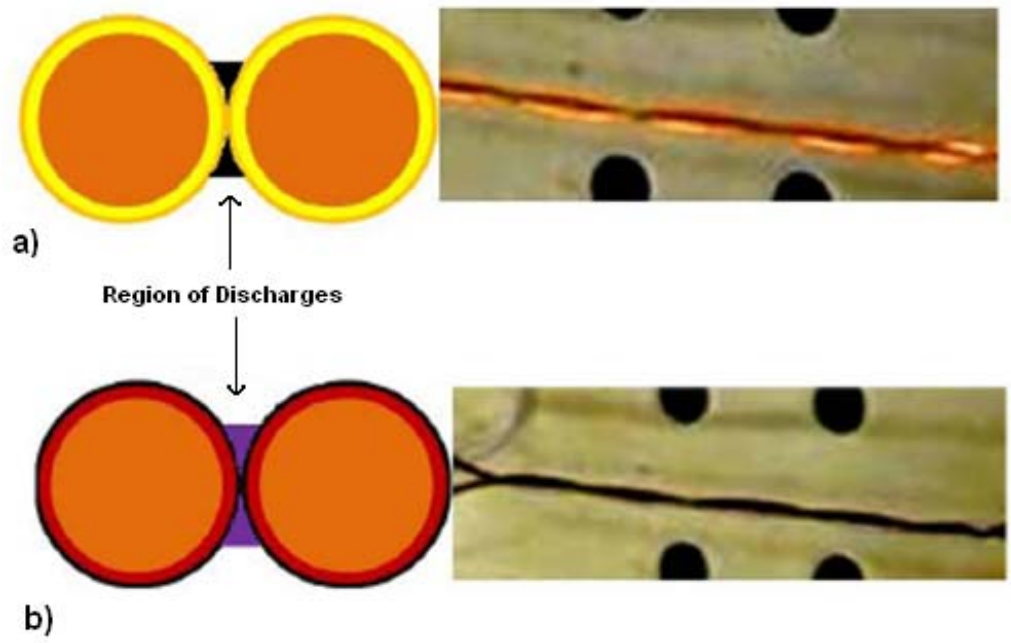

Figure 7.29 Comparison between machine windings a) before aging b) after aging

For no aging, the region of discharge is the narrow air gap between the insulations. Ionization occurring in the air gap causes an increase of insulation surface conductivity. The changes in the insulation permittivity for aged samples also have an impact on the electrical field distribution around the air gap. For the first 100 hrs of

accelerated aging, the breakdown voltage and PDIV of the insulations are observed to increase. After 100 hrs, breakdown voltage and PDIV decreases. This observation leads to an expectation of change in the surface condition of the machine winding insulation, as shown in Figure 7.29. This change in surface condition is at first non-uniform, until after 100 hrs when it begins to become more uniform [41-43].

7.3 Simulation of Electric Field Distribution

To verify the effect of changing surface conductivity and permittivity in the breakdown voltage of the insulation, a simulation model is developed for the twisted pair of sample using Ansoft 2D Maxwell software. Figure 7.30 shows the configuration model of the twisted pair cross section. The wire cross section in the model is assumed to be circular, which indicates that software analyzes it as an infinite cylinder. The model is prepared with a 14 AWG size round conductor with a heavy build insulation. The diameter of the copper wire is chosen to be 1.62 mm with insulation thickness of 0.05 mm. The two wires of the twisted sample are symmetric about the origin with an air gap in between them. The section of the insulation near the contact is designed with 0.002 mm thickness to simulate the model with increased surface conductivity. The polyimide insulation (ε_r=2.6) and the polyester insulation (ε_r=4.8) with a polyamideimide layer (ε_r = 2.8) are selected for the simulation, which corresponds to MW16-C and MW 35-C machine winding respectively.

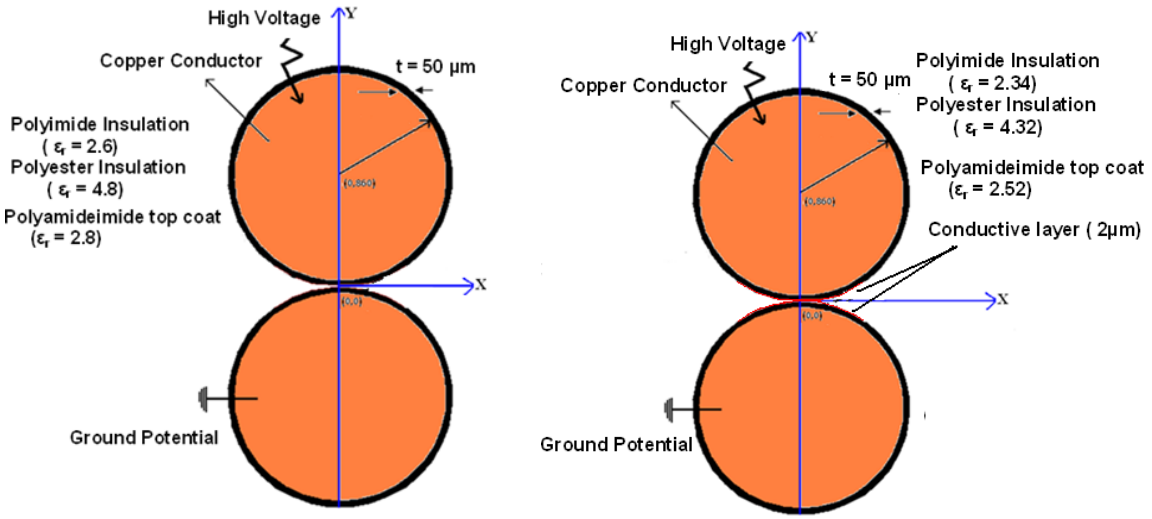

a) b)

Figure 7.30 Simulation model of cross-section area of twisted pair of sample a) before aging b) after aging

7.4 Simulation Results

At an applied effective test voltage of about 0.7 kV, the E-field in the air gap between the wires exceeds that of Paschen minimum (3.27 kV/mm) and partial discharge inception occurs. Two models are developed corresponding to the sample before and after accelerated aging.

The nominal applied voltage during the partial discharge inception voltage is around 700V. In order to compare the simulation results directly to the change in surface conductivity and relative permittivity, the peak value is of interest. The peak voltage of 990V is applied to the one conductor while the other conductor in the twisted pair is at ground potential. The simulation results are calculated for both polyimide insulation and polyester insulation with polyamideimide top coat and presented in Figure 7.31.

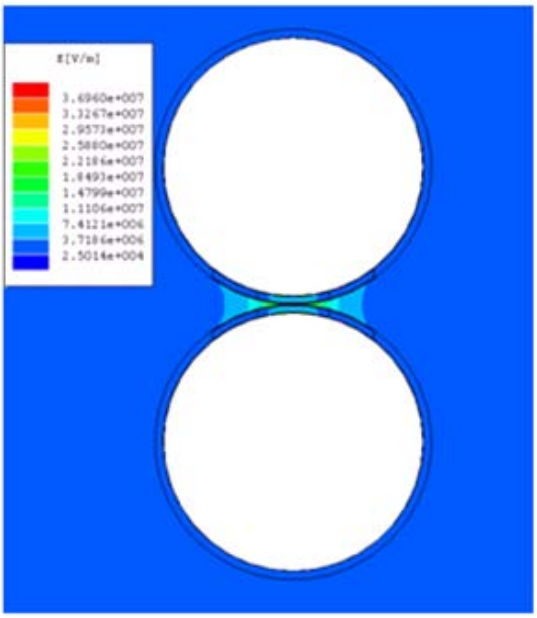

a)

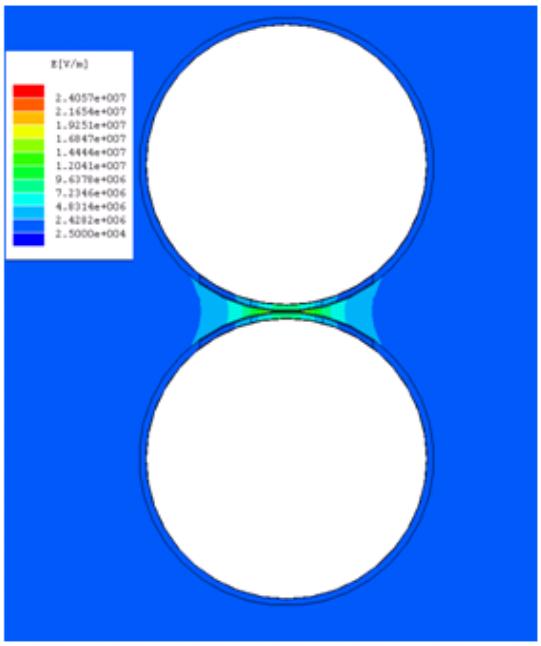

b)

Figure 7.31 Electric field distribution of new sample a) MW 35-C b) MW 16-C

From the simulation results, it is observed that the maximum field strength in MW 35-C insulation (polyester layer with polyamideimide top coat) is 36.9kV/mm; whereas, the maximum field strength in MW 16-C insulation (polyimide) is 24kV/mm. Therefore, the electric filed distribution in the twisted pair of sample configuration depends on the relative permittivity of the material. The Paschen minimum value in case of polyimide insulation is extended beyond that of polyester insulation to incorporate a wide region of discharges. This is the possible reason for having a higher breakdown voltage for MW 16-C than MW 35-C.

The second model is assumed to have increased conductivity and changed permittivity, which is expected to happen due to ionization and partial discharge activity. For epoxy resin, the effective surface conductivity under partial discharge activity after certain hours should be higher than the one measured before aging without partial discharge (~10-9 S/m) [42]. From this information, conductivity of the contacted surface (region of ionization) is assumed to be around 10^{-9} S/m with 10% decrease in relative permittivity after 100 hrs of accelerated aging. These assumptions are applied to both simulation conditions for polyester and polyimide insulation. The simulation results for the aged sample for certain duration is shown in Figure 7.32.

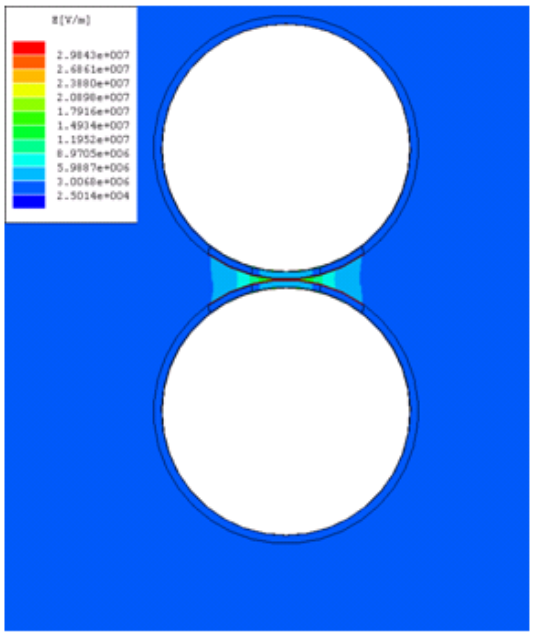

a)

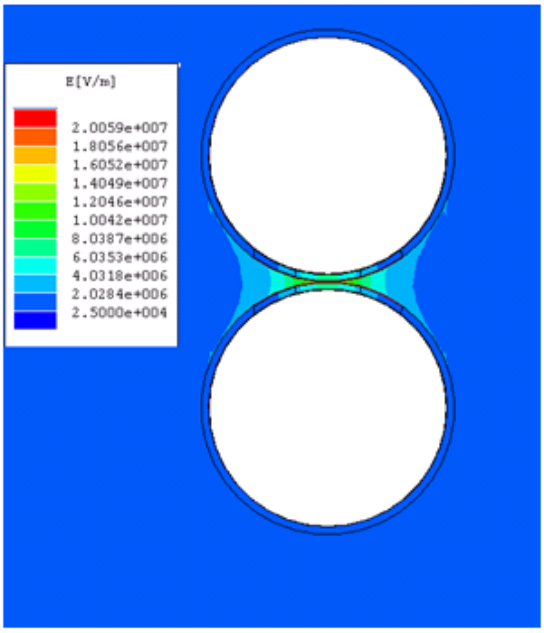

b)

Figure 7.32 Electric field distribution of aged sample with relative change in surface conductivity and permittivity a) MW 35-C b) MW 16-C

The simulation results show that maximum electric field strength in the configuration become 29.8kV/mm for MW 35-C and 20kV/mm for MW 16-C after increase in surface conductivity. The region of the discharges (Paschen minimum) extends further for polyimide insulation. This observation is contributed to the possible increase in breakdown voltage after 100 hrs of accelerated aging condition, as verified by experimental results. Generally, conductivity is found to have already attained its saturation values after certain period of degradation [42]. Thus, a longer period of accelerated aging results in lower values of breakdown voltage

CHAPTER VIII

CONCLUSION

In the presented results, comparable 60 Hz ac breakdown measurements are performed for NEMA 16-C insulation. In addition, change in partial discharge (PDIV and PDEV) and breakdown voltage are monitored versus the accelerated aging with high frequency pulse voltage and high temperature. The evaluated machine winding insulations are NEMA MW 80-C (polyurethane-nylon material), NEMA MW 35-C (polyester material with a polyamideimide coating), NEMA MW 16-C (a polyimide resin), and NEMA 73-C (polyester –amide-imide top coat). The main conclusions from the measurement could be stated as;

- 60 Hz ac accelerated aging showed that time to breakdown can be modeled by combining the Weibull distribution of failure data with the inverse power law and the Arrhenius equation with respect to test voltage and temperature.
- When performing accelerated voltage aging of twisted pairs of wires, a large partial discharge activity in the air gap between the insulated wires became a dominant aging mechanism, causing rapid breakdown at the highest voltages.
- The time to breakdown needs to be measured at the lowest possible voltage to enhance the lifetime characteristic under service conditions.

- Partial discharge measurements taken after accelerated aging (with high frequency pulse voltage and temperature) for the MW 35-C type of insulation shows higher partial discharge inception voltage and partial discharge extinction voltage due to the partial discharge resistant polyamideimide coating. The measured PDIV and PDEV for the MW 35-C are higher compared to the data for MW 80-C, MW 16-C, and MW 73-C.
- High temperature resistance and high quality polyimide in MW 16-C causes it to have the highest breakdown strength. The variation of breakdown voltage with 1000 hrs of accelerated aging shows relatively small change for polyimide insulation, mainly owing to its high thermal resistance properties.
- The MW 35-C, MW 16-C, and MW 73-C show an extended life period after 500 hrs of accelerated aging. As the MW 35-C has a partial discharge resistant layer, there is less surface discharge and therefore, the MW 35-C insulation has longer life than MW 80-C under the same accelerated aging conditions.
- There is an increase in partial discharge inception voltage, partial discharge extinction voltage, and breakdown voltage for a sample accelerated aged in the first 100 hrs. The increase in the measured data is interpreted as a temporary improvement in the electrical insulation condition cause by possible increase in the conductivity on the surface and microvoids of the insulation.
- The simulation results are obtained for the cross section area of the twisted pair of samples. The simulation results show a change in electric field strength in the air gap

due to change in conductivity and relative permittivity for NEMA 16-C and NEMA 35-C machine winding insulation.

The possible future work could be;

- Application of multi-stress for accelerated degradation of the machine winding insulation for new materials like Enamel, Mylar, and Mica.
- Determine the constants of multi-stress model considering the effect of high frequency pulse voltage and temperature for the insulations.
- Develop machine winding insulation breakdown model considering partial discharge phenomena.

REFERENCES

[1] E. Sugimoto, "Application of Polyimide Films to the Electrical and Electronic Industries in Japan." *IEEE Electrical Insulation Magazine*, vol-5, pp.15-23, 1989.

[2] G. C. Stone, et al., "Inverter Fed Drives: Which Motor Stators are at Risk," *Industry Application Magazine, IEEE*, Vol. 6, pp 17-22, 2000.

[3] Eyad Abu-Al-Feilat, "Lifetime Characteristics of Magnet Wires under High Frequency Pulsating Voltage and High Temperature" PhD Dissertation, Mississippi State University, 2000.

[4] E.A. Feilat, S. Grzybowski, P. Knight, "Accelerated Aging of High Voltage Encapsulated Transformers for Electronics Applications," *Proceedings of the 6th International Conference on Properties and Application of Dielectric Materials*, Vol. 1, pp. 209-212, 2000.

[5] E.A. Feilat, S. Grzybowski, P. Knight, "Electrical Aging Models for Fine Gauge Magnet Wire Enamel of Flyback Transformer," *Proceedings of the IEEE Southeast Conference*, pp. 146-149, 2000.

[6] S. Grzybowski, S. Bandaru, "Effect of Frequency, Temperature, and Voltage on the Lifetime Characteristics of Magnet Wires under Pulse Voltage," *Proceeding of the IEEE International Conference on Solid Dielectrics, ICSD'2004*, Vol. 2, pp. 876-879, 2004.

[7] S. Grzybowski, N. Kota, "Lifetime Characteristics of Magnet Wires under Multistress Conditions," *Conference on Electrical Insulation and Dielectric Phenomena (CEIDP'2005)*, Nashville, TN, pp. 605-608, 2005.

[8] S.Grzybowski, A. Mani, and C.D. Taylor, "Partial Discharge Patterns of Magnet Wire Samples under Voltage Stresses," *2005 Annual Report Conference on Electrica Insulation and Dielectric Phenomena (CEIDP'2005)*, Nashville, TN, pp. 422-425, 2005

[9] S.Grzybowski, C.D. Taylor, S.R. Chalise, "Electrical Degradation Study of Machine Winding Insulation," *Proceedings of International Conference on High Voltage Engineering and Application*, November 9-12, 2008, Chongqing, China, pp. 321-325.

[10] S.R.Chalise, S. Grzybowski, and C. D. Taylor, "Accelerated Electrical Degradation of Machine Winding Insulation," *Proceedings of IEEE Electrical Ship Technologies Symposium*, April 20-22, Baltimore, Maryland, pp. 533-538, 2009.

[11] S.R Chalise, S.Grzybowski, C.D. Taylor," Accelerated Electrical Degradation of Machine Winding Insulation," *Accepted for North America Power Symposium (NAPS, 2009)*, Mississippi State University, Oct 4-6, 2009.

[12] M. Hatada, S. Amano, T. Sawamoto, and k. Ueda, "Frequency Characteristics of Magnet Wires", *Proceedings of Electrical and Electronics Insulation Conference*, Rosemont, Illinois, Oct. 4-7, pp. 485-488, 1993.

[13] J.A. Oliver, and G. C. Stone, "Implications for the Application of Adjustable Speed Drive Electronics to Motor Stator Winding Insulation," *IEEE Electrical Insulation Magazine*, Vol. 11, No. 4, July-Aug, pp. 32-36, 1995.

[14] A. H. Bonnett, "Analysis of the Impact of Pulse-Width Modulated Inverter Voltage Waveform on AC Induction Motors," *IEEE Transaction on Industry Application*, Vol. 32, No. 2, pp. 386-392, 1996.

[15] M. Melfi, A. M. Jason Sung, S. Bell, and G. L. Skibinski, "Effect of Surge Voltage Risetime on the Insulation of Low-Voltage Machines Fed by PWM Converters," *IEEE Transaction on Industry Application*, Vol. 34, No. 4, pp. 766-775, 1998.

[16] D. Fabiani, G. C. Montanari, A. Cavallini, and G. Mazzanti, "Relation Between Space Charge Accumulation and Partial Discharge Activity in Enameled Wires Under PWM-like Voltage Waveforms," *IEEE Transaction on Dielectric and Electrical Insulation*, Vol. 11, No. 3, pp. 393-405, 2004.

[17] G. C. Stone, I. M. Culbert, and B. A. Lloyd, "Stator Insulation Problems Associated with Low Voltage and Medium Voltage PWM Drives," *IEEE Technical Conference Record of Cement Industry*, April 29- May 2, pp. 187-192, 2007.

[18] C. Hudon, N. Amyot, T. Lebey, P. Castelan, and N. Kandev, "Testing of Low-Voltage Motor Turn Insulation Intended for Pulse-Width Modulated Application," *IEEE Transaction on Dielectric and Electrical Insulation*, Vol. 7, No. 6, pp. 783-789, 2000.

[19] P. H. F. Morshuis, "Degradation of Solid Dielectrics Due to Internal Partial Discharge: Some Thought on Progress made and Where to Go Now," *IEEE Transaction on Dielectrics and Electrical Insulation*, Vol. 12, No. 5, pp. 905-913, 2005.

[20] E. Kuffel, W. S. Zaengl, and J. Kuffel, "High Voltage Engineering: Fundamentals," Second Edition 2000, Butterworth-Heinemann, Oxford, UK.

[21] A. H. Bonnett, and G. C. Soukup, "Cause and analysis of stator and rotor failures in three-phase squirrel-Cage Induction Motors," *IEEE Transaction on Industry Applications*, Vol. 28, No. 4, pp. 921-937, 1992.

[22] A. C. Gjerde, "Multifactor Ageing Models – Origin and Similarities," *IEEE Electrical Insulation Magazine*, Vol. 13, No. 1, pp. 6-13, 1997.

[23] B. K. Gupta, B. A. Lloyd, G. C. Stone, S. R. Campbell, D. K. Sharma, and N. E. Nilsson, "Turn Insulation Capability of Large AC Motors Part 1- Surge Monitoring," *IEEE Transaction on Energy Conversions*, Vol. EC-2, No. 4, pp. 658-665, 1987.

[24] R. H. Rehder, "Preliminary Evaluation of Motor Insulation for Variable Speed Applications," *Proceedings of Electrical Electronics Insulation Conferences and Electrical Manufacturing and Coil Winding Conference, EEIC/ICWA Exposition*, 4-7 Oct., Chicago, pp. 333-336, 1993.

[25] M. Kaufhold, "Failure Mechanism of the Interturn Insulation of Low Voltage Electric Machines Fed by Pulse Controlled Inverters," *Annual Report Conference on Electrical Insulation and Dielectric Phenomena (CEIDP'1995),* 22-25 Oct, pp. 254-257, 1995.

[26] G. Skibinski, J. Erdman, and J. Campbell, "Assessing AC Motor Dielectric Withstand Capability to Reflected Voltage Stress Using Corona Testing," *Conference Record of Industry Application*, Vol. 1, pp. 694-702, 1996.

[27] W. Yin, "Dielectric Properties of an Improved Magnet Wire for Inverter-Fed Motors," *IEEE Electrical Insulation Magazine*, Vol. 13, No. 4, pp. 17-23, 1997.

[28] D. Fabiani, G. C. Montanari, and A. Contin, "Aging Acceleration of Insulating Materials for Electrical Machine Windings Supplied by PWM in the Presence and in the Absence of Partial Discharge," *Proceedings of the 7th International Conference on Solid Dielectrics*, Eindhoven, the Netherland, pp. 283-286, 2001.

[29] W. Yin, K. Bultemeier, D. Barta, and D. Floryan, "Improved Magnet Wire for Inverter-Fed Motors," *Proceedings of Electrical Insulation Conference, and Electrical Manufacturing and Coil Winding Conference*, 22-25 Sept., pp. 379-382, 1997.

[30] S. U. Haq, S. H. Jayaram, and E. A. Cherney, "Performance of Nanofillers in Medium Voltage Magnet Wire Insulation under High Frequency Applications," *IEEE Transaction on Dielectrics and Electrical Insulation*, Vol. 14, No. 2, pp. 417-426, 2007.

[31] ReliaSoft, *Weibull++ Life Data Analysis Reference Version 7.0*, Tuscan, Arizona, USA.

[32] E. Ildstad, and S. R. Chalise, "AC Voltage Endurance of Polyimide Insulated Magnet Wire," *Submitted for Conference on Electrical Insulation and Dielectric Phenomena (CEIDP, 2009)*, 18-21 Oct., Virginia, USA.

[33] P. Cygan, and J. R. Laghari, "A Review of Electrical and Thermal Multistress Aging Models," *Conference Record of the IEEE International Symposium on Electrical Insulation*, pp. 15-20, 1990.

[34] G. C. Montanari, and M. Cacciari, "A Probabilistic life Model for Insulating Materials Showing Electrical Thresholds", *IEEE Transaction on Electrical Insulation*, Vol. 24, No. 1, pp. 127-134, 1989.

[35] J.C. Devins, "The Physics of Partial Discharge in Solid Dielectrics," *IEEE Transaction on Electrical Insulation*, Vol. 19, pp. 475-495, 1984.

[36] IEC Standard 60270 (Third Edition, 2000). Partial Discharge Measurements. International Electro technical Commission (IEC), Geneva, Switzerland.

[37] ANSI/NEMA MW 1000-2003, Revision 3, 2007, Magnet wire, part 3.

[38] http://www.mwswire.com/awgsearch1.asp

[39] IEC Std. 62068: *Evaluation of electrical stresses produced by repetitive impulses*. Part 1: *General methods of evaluation of electrical endurance* (IEC 98-160 CDV). Part 2: *State of the art report* (62068-2 (2001-08)).

[40] G.Rabilloud, "High-Performance Polymers 3. Polyimide in Electronics Chemistry and Applications." *T Editions Technip*, Paris, 2000.

[41] X. Guo, G. Wu, K. Zhiou, B. Gao, and J. Wu," Influence of inorganic nano-filler to partial discharge of polyimide film under high frequency impulses," *International Conference on Condition Monitoring and Diagnosis*, Beijing, China, pp.1226-1229, 2008.

[42] C. Hudon, R. Bartnikas, and M.R. Wertheimer, "Spark-to-glow discharge transition due to increased surface conductivity on epoxy resin specimens," *IEEE Transaction on Dielectric and Electrical Insulation*, Vol.28, No.1, 1993, pp. 1-8.

[43] K. Wu, T. Okamoto, and Y. Suzuoki, " Effects of discharge area and surface conductivity on partial discharge behavior in voids under square voltages," *IEEE Transaction on Dielectric and Electrical Insulation*, Vol. 14, No. 2, pp 461-470, 2007.